Bioaffinity Screening with a Rapid and Sample-Efficient Autosampler for Native Electrospray Ionization Mass Spectrometry

Journal Article

Author(s):
Kaeslin, Jérôme; Brunner, Cyrill; Ghiasikhou, Sahar; Schneider, Gisbert (iD); Zenobi, Renato (iD)

Supporting Information

Bioaffinity Screening with a Rapid and Sample-Efficient Autosampler for Native Electrospray Ionization Mass Spectrometry

Jérôme Kaeslin[†], Cyrill Brunner[†], Sahar Ghiasikhou[†], Gisbert Schneider[†], and Renato Zenobi[*,†]

[†] Department of Chemistry and Applied Biosciences, ETH Zürich, Vladimir-Prelog-Weg 3, CH-8093, Switzerland

Table of contents

EXPERIMENTAL SECTION FOR TSA AND SPR

Sample preparation for TSA. A **P** solution was prepared at a concentration [**P**] = 4 µM, which was quantified with a spectrophotometer (Shimadzu BioSpec) controlled by the corresponding software (BioSpec Nano v. 2.0). SYPRO Orange was used at 5x stock concentration. Both the **P** and dye were dissolved in 10 mM PBS with 3% or 5% DMSO, respectively.

For the ligands from table S1, every **L** was prepared as 50 mM solution in DMSO and diluted to 1 mM with 10 mM PBS. This solution was further diluted with 10 mM PBS onto a 96-well microplate to a final concentration of 250 µM in 10 mM PBS with 5% V/V DMSO. Final volumes were 10 µl **P** solution, 5 µl dye and 5 µl **L** solution. For **A23-A27** and the MS-binding ligands from table S2, every **L** was prepared as 100 mM solution in DMSO and diluted to two concentration on the 96-well microplate; 10 µM and 100 µM, both in 10 mM PBS with 3% V/V DMSO. Final volumes were 10 µl **P** solution, 5 µl dye and 5 µl **L** solution. Samples were incubated for 15 min at room temperature.

Thermal shift assay. For the ligands from table S1, the **P** alone (**L** absent), was measured as non-ligand control (NLC) five times. Every **L** alone (**P** absent) was measured once to determine **L**'s fluorescence. Every **P**+**L** pair was measured in duplicate. For **A23-A27** and the MS-binding ligands from table S2, the **P** alone (**L** absent), was measured as NLC six times. Every **L** alone (**P** absent) was measured three times to determine **L** fluorescence. Every **P**+**L** pair was measured in triplicate. The dye alone was measured six times.

All experiments were performed in 30 µl cone-bottom transparent 96 well plates on a StepOne Plus Real Time PCR System (Applied Biosystems, Waltham, USA). The screening and quantitative evaluation were performed at a heating rate of 1 K min^{-1} and 0.5 K min^{-1}, respectively, with 2 min and 4 min hold time, respectively, at 25 and 99 °C. Thermal Shift Assay experiments were performed with the StepOne control software (v. 2.3, Applied Biosystems, Waltham, USA) and data analyzed with Microsoft Office Excel 365 (Microsoft Corp., Seattle, USA). Data was plotted with GraphPad Prism. (v. 8.3.0, GraphPad Software, San Diego, USA). Inflection temperatures T_M of each condition were calculated from the minimum of the first negative derivative computed by the StepOne software. Difference in melting temperature ΔT_M of a [**P**+**L**] complex was calculated by subtraction of the complex T_M and NLC T_M average:

$$\Delta T_{M,[P+L]} = T_{M,[P+L]} - \overline{T_{M,NLC}}$$

Sample preparation for SPR. A **P** solution was prepared at a concentration [**P**] = 20 µg ml^{-1}, which was quantified with the same procedure as for TSA. For qualitative screening, ligands (table S1, **A** ligands) were dissolved in DMSO and diluted to 50 µM in PBS-T with 5% V/V DMSO. Likewise for quantitative screening, most ligands (table S1; **A23-A27**, table S2; **B** ligands) were prepared in a twelve-point dilution series ranging from 500 µM to 2 nM in PBS-T with 3% V/V DMSO expect for **A29**, **A105-A107** and **A110-A111**, which were dissolved in 5% V/V DMSO.

Surface Plasmon Resonance. SPR-experiments were performed with the Sierra Controller (v. 2.4., Bruker Daltonics, Hamburg, Germany) and data analyzed and sensorgrams plotted with Sierra Analyser (v. 3.1.34, Bruker Daltonics, Hamburg, Germany). Other plots were generated with GraphPad Prism (v. 8.3.0, GraphPad Software, San Diego, USA).

The surface was activated with a mixture of 100 mM NHS and 400 mM EDC injected with a flow rate of 5 µl min^{-1} for 8 min over both measurement spots A+B. Subsequently, the 20 µg ml^{-1} **P** solution was injected for 6 min contact time with 25 µl min^{-1} over spot B. A final immobilization level of 4000 RU was targeted. A 1 M ethanolamine solution was injected at a flow rate of 5 µl min^{-1} to inactivate the surface for 8 min over both measurement spots A+B. The immobilization and sensor preconditioning were performed in 10 mM PBS buffer with 0.05% Tween20 (PBS-T).

The system was equilibrated with the assay buffer (10 mM PBS + 0.05% Tween20 + 5% DMSO). First, the functionality of the **P** was assessed by determining the dissociation constant of 50 µL of the positive control compound **A23** with eight concentrations (100 µM to 10 nM) with a flow rate of 25 µL min^{-1} and a 120 s dissociation time in a single injection cycle kinetics format (one concentration per channel). Each injection of **A23** was preceded by a buffer injection (50 µL, 25 µL min^{-1}, 120 s dissociation time). Additionally, **A23** and **A24** were injected at 50 µM on all channels (50 µl, 25 µl min^{-1}, 60 s). Each measurement of a compound dilution series was preceded and followed by five DMSO controls with contents of 4.6% to 5.4% (50 µl at 25 µl min^{-1}). All experiments were performed at 25°C.

For qualitative screening, all compounds (**A1-A111**) were measured at 50 µM with 2 min contact time at a flow rate of 25 µL min^{-1} and 60 s dissociation time except **A98**, which was insoluble in this concentration range. Each injection of analyte was preceded by a buffer injection (50 µL, 25 µL min^{-1}, 60 s dissociation time). Compounds **A23** and **A27**, **A29** and **B16** were used as positive controls, compounds **A24-A26** and **A28** as negative controls. Intermittent injections of the **A23** and **A24** were used to assess potential changes to the immobilized **P**. The data was analyzed by "double subtraction", i.e., subtraction of the reference surface and buffer injections from the raw data. The obtained equilibrium signal was normalized by the MW (first quotient) of the compound and immobilization level of **P** (second quotient) according to:

$$R_{norm} = \frac{R_{det, \text{ channel } x}}{MW_L} \cdot \frac{R_{immob P, \text{ highest}}}{R_{immob P, \text{ channel } x}}$$

For quantitative screening, the binding affinities of compounds **A23-27**, **A29**, **A105-107**, **A110-111**, **B3**, **B6**, **B9**, **B13**, **B16**, **B19**, **B22** and **B28** to **P** were determined by SPR with the same approach. Compounds **A29**, **A105-107** and **A110-111** were measured in PBS-T supplemented with 5% DMSO, the other compounds with 3% DMSO supplementation. All experiments were performed in identical conditions with respect to temperature, and immobilization of **P**. All compounds were measured from the weakest to the strongest binding compound and sufficiently long dissociation time such that no regeneration was necessary. Furthermore, all compounds were measured four times at 25 µl min^{-1} flow rate with 50 µl volume (i.e., 2 min contact time) and with a minimum of 120

seconds dissociation time. Each compound-injection was preceded and proceeded by a buffer injection (50 µl at 25 µl min^{-1}, min. 120 s dissociation time). All experiments were performed at 25°C. The data was analyzed by "double subtraction" as described above.
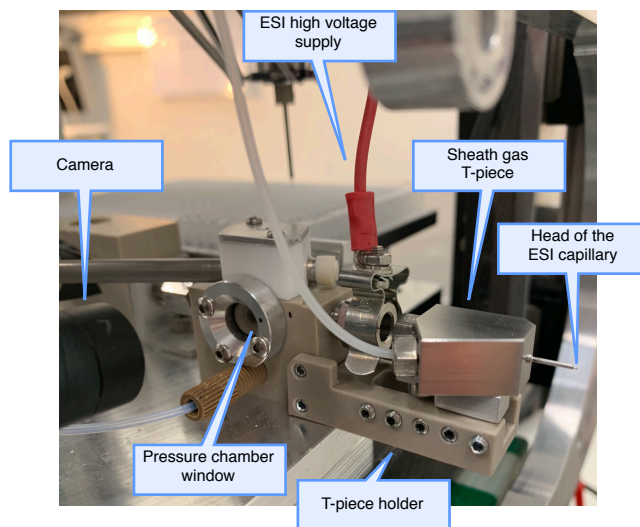
Figure S3. Gap sampler modifications: important parts are labeled. The camera, the pressure chamber and the ESI high voltage supply were already used in the original design.[1] In this study, a coaxial sheath gas was installed. For this purpose, a metallic T-piece was used to circulate gas around the ESI capillary. The sheath gas was $250\,\mathrm{l\,h^{-1}}$ N_2 from the mass spectrometer's purge gas supply. The T-piece was held by a PEEK machined holder, which itself was attached to the pressure chamber.
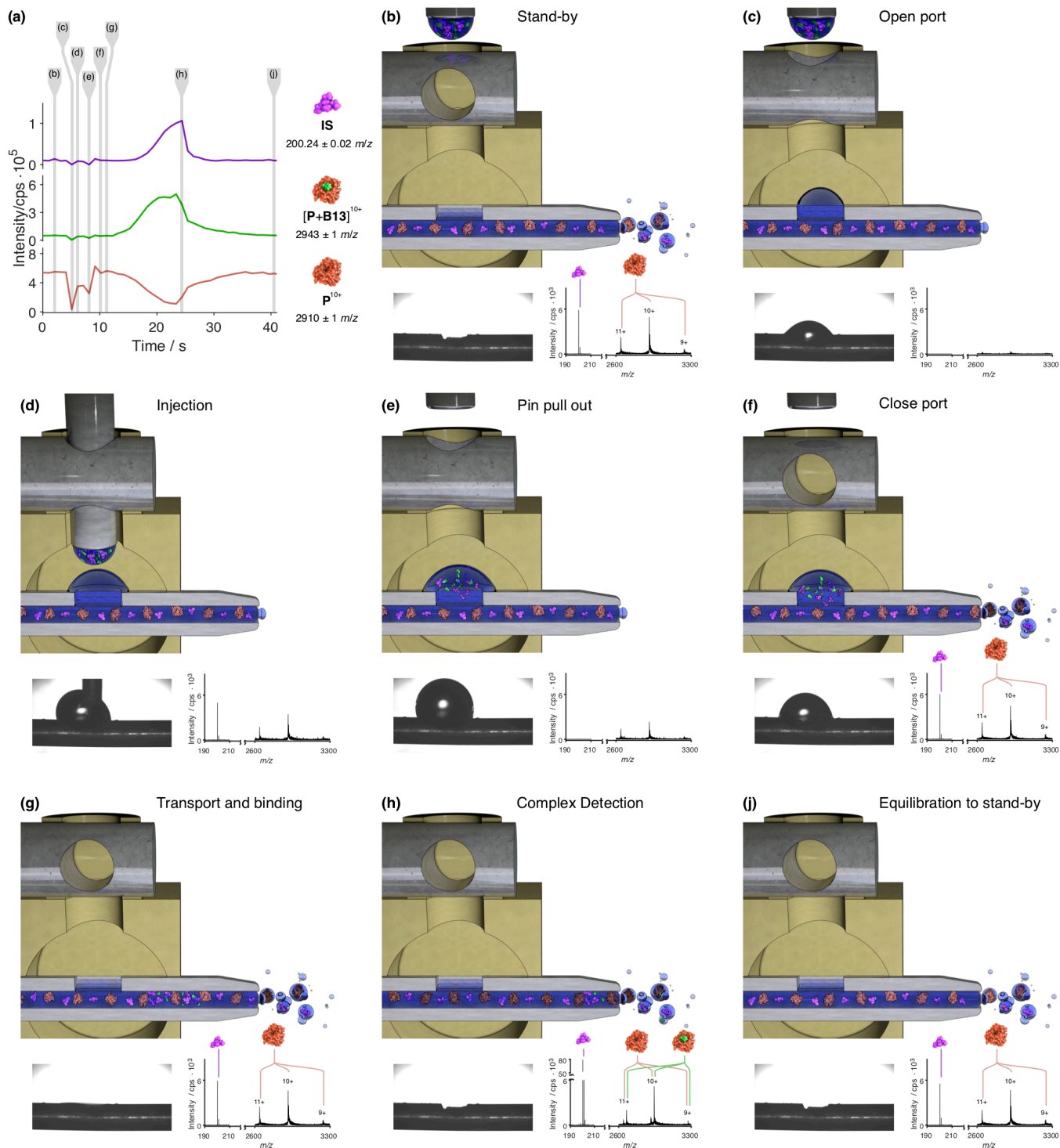
Figure S4. Overview of one injection cycle. As an example, the injection of **B13** is shown. (a) shows the XIC of the internal standard **IS**, of the complex $[\mathbf{P}+\mathbf{B13}]^{+10}$ and three free protein $\mathbf{P}^{+10}$ before, during and after injection. The different time points which are shown in the subsequent subfigures are highlighted with a grey line. (b) Schematically shows the state of the gap sampler prior to injection. There, the open capillary is continuously fed with **P** and **IS** while the pin picked up the solution containing **L** and **IS** from the well plate. In the photograph of the open capillary, the hole on the capillary's top is visible. In the continuously recorded mass spectrum, different charge states and adducts of **P** are observed together with the singly charged **IS**. (b) The injection starts by opening the pressure port. This causes a flooding of the feed solution such that a droplet is formed on the top of the open capillary as can be recognized in the photograph and drawing. Meanwhile, the electrospray vanishes such that no more mass spectra are acquired. This causes an intensity drop in the XIC. (d) The **L** and **IS** containing hanging droplet is injected into the droplet on the capillary's top. (e) The pin is removed from the pressure chamber. (f) The chamber port is closed. The overpressure reestablishes and pushes the droplets back into the open capillary. As a result, the electrospray restabilizes such that the **IS** and **P** signals are again observed in the spectrum. (g) The system stabilizes, and the ligands are flushed towards the end of the capillary. During these few seconds of residence time, the ligand binds to the protein eventually. (h) When the injected **IS** and **L** arrive at the capillary's end, an **IS** signal increase is observed. With this standard addition of the **IS**, the maximum **IS** concentration $[\mathbf{IS}]_{max}$ can be quantified. With the known ratio r of **L** to **IS** in the injection solution, the maximum **L** concentration $[\mathbf{L}]_{max}$ can be calculated:

$[\mathbf{L}]_{\max} = r([\mathbf{IS}]_{\max} - [\mathbf{IS}]_{\text{fed}})$, where $[\mathbf{IS}]_{\text{fed}}$ is the **IS** concentration in the feed solution. The intensity ratio of bound to unbound protein $\overline{R} = I([\mathbf{P} + \mathbf{Ac}_q + \mathbf{L}]^{+n})/I([\mathbf{P} + \mathbf{Ac}_q]^{+n})$ is read out from the mass spectrum where this ratio is highest (not shown, one scan before (h)). This ratio is assumed arise from the concentration $[\mathbf{L}]_{\max}$. Knowing $[\mathbf{L}]_{\max}$, $\overline{R}$ and the fed protein concentration $[\mathbf{P}]_0$, the K_D can be calculated. (j) The system equilibrates and is ready for the next injection. Potential carryover could be recognized when the $[\mathbf{P}+\mathbf{L}]^{+10}$ and $\mathbf{P}^{+10}$ XICs don't reach their pre-injection intensities. However, except for compound **A29** in figure S5, this was never an issue.
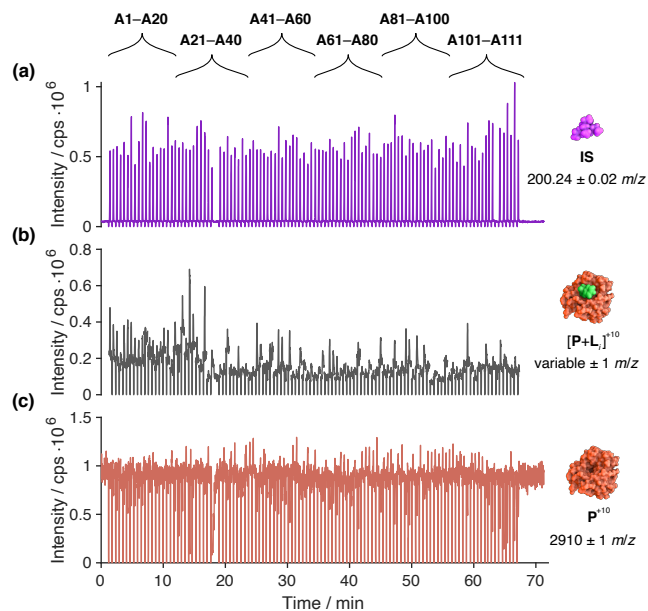
Figure S5. Qualitative screening of the **A1-A111** ligand set with one repetition. 3 mM **L** and 600 µM **IS** were dissolved in 94:6 DMSO:buffer. This solution was injected into a 2:98 DMSO:buffer feed containing 3 µM **P** and 0.5 µM **IS**. The average injected $[\mathbf{L}]_{max}$ is estimated at 37 µM (not quantified due to ion suppression). (a) shows the XIC of the **IS**, which was present both in the feed as well as in the injected solution. (b) The XIC at the *m/z*, where the complex $[\mathbf{P+L}]^{+10}$ would be observable if a binder was injected. **A29** was binding but precipitates in the open capillary. Therefore, a washout was required before the next ligand **A30** was injected. (c) shows the XIC of the unbound $\mathbf{P}^{+10}$. **A98** was later removed from the set because it was not soluble in concentrations needed for TSA and SPR experiments.
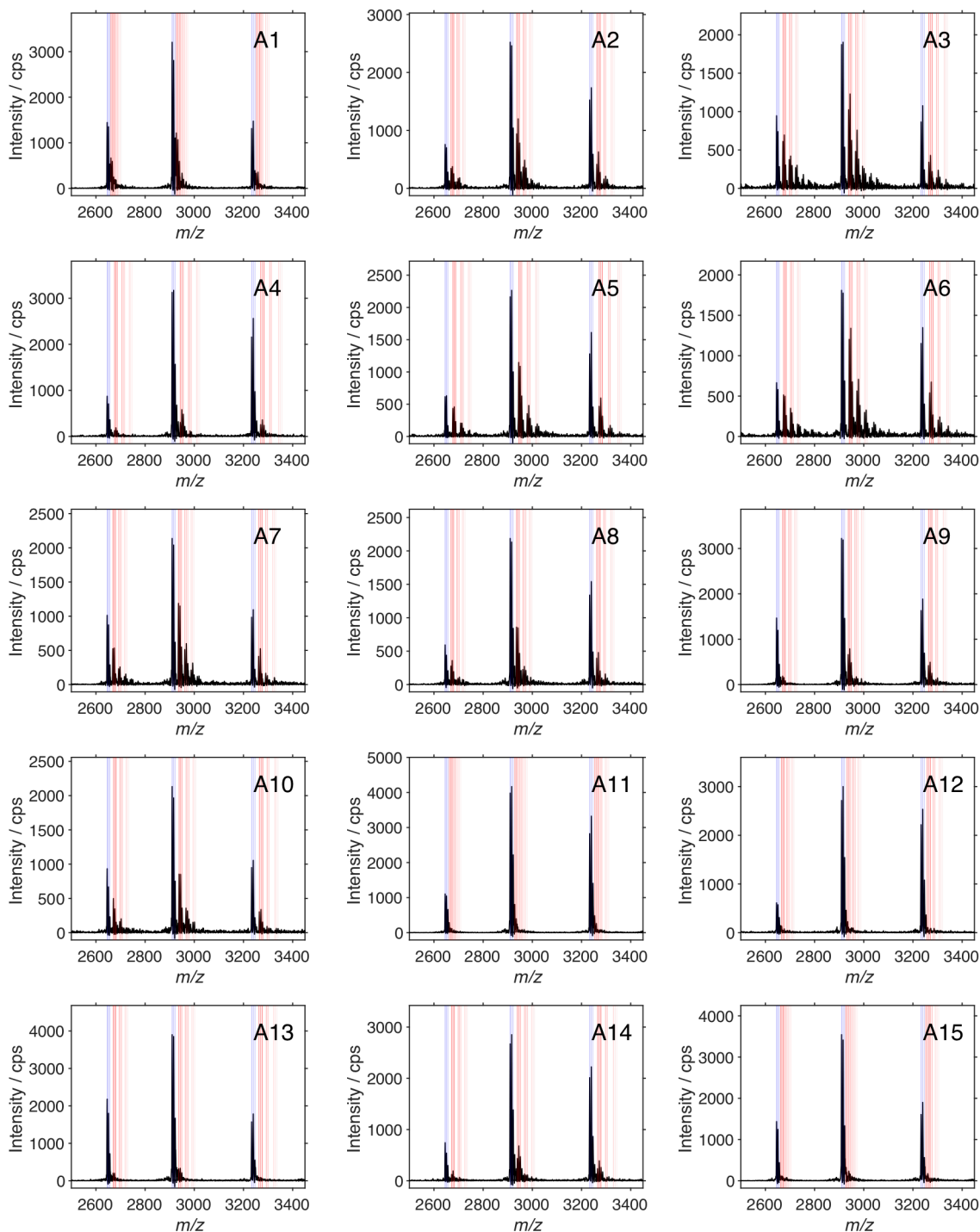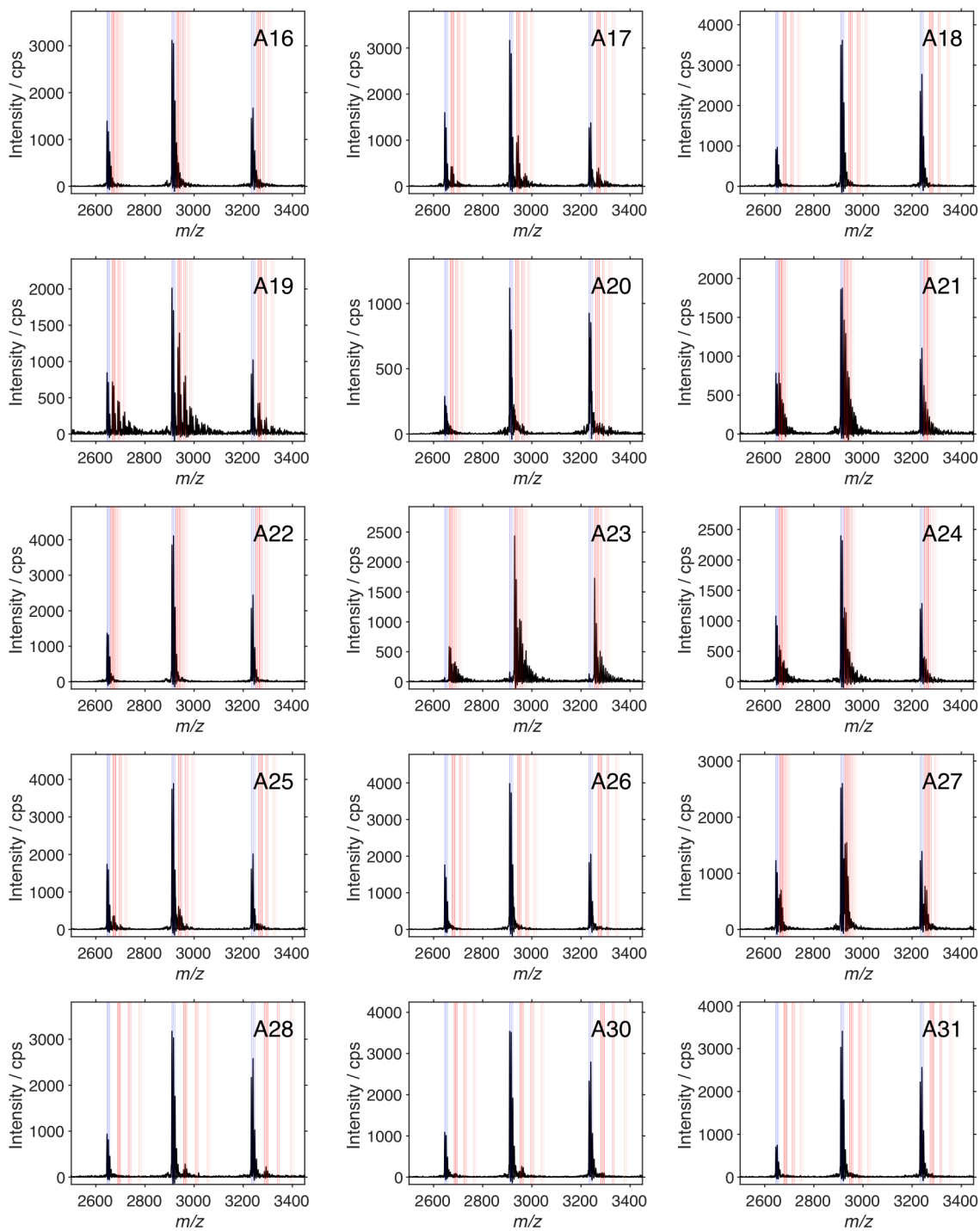
Figure S6. Mass spectra acquired for the qualitative screening of the ligands **A1** to **A111**. The shown spectra have the highest ratio $\overline{R} = \overline{I([\mathbf{P} + \mathbf{Ac}_q + \mathbf{L}_p]^{n+})/I([\mathbf{P} + \mathbf{Ac}_q]^{n+})}$ during one injection cycle (see figure S4), where $q=0,1,2$ are acetate adducts and $p=1,2,3$ represent specific or non-specific **L** binding. Thus, the shown spectra were acquired only for 1 s. They were smoothed and baseline subtracted. The red (bound) and the blue (unbound) rectangles mark the integration limits for +11, +10 and +9 charge states of $\mathbf{P}^{+n}$, $[\mathbf{P}+\mathbf{Ac}]^{+n}$, $[\mathbf{P}+\mathbf{Ac}_2]^{+n}$, $[\mathbf{P}+\mathbf{L}]^{+n}$, $[\mathbf{P}+\mathbf{Ac}+\mathbf{L}]^{+n}$, $[\mathbf{P}+\mathbf{Ac}_2+\mathbf{L}]^{+n}$, $[\mathbf{P}+\mathbf{L}_2]^{+n}$, $[\mathbf{P}+\mathbf{Ac}+\mathbf{L}_2]^{+n}$, $[\mathbf{P}+\mathbf{Ac}_2+\mathbf{L}_2]^{+n}$, $[\mathbf{P}+\mathbf{L}_3]^{+n}$, $[\mathbf{P}+\mathbf{Ac}+\mathbf{L}_3]^{+n}$, $[\mathbf{P}+\mathbf{Ac}_2+\mathbf{L}_3]^{+n}$ which are used to determine the calculatory-K_D value. The spectrum for **A29** is not shown because it precipitates in the open capillary. However, it bound the protein clearly (Figure S5) and therefore a washout was required. **A98** was later removed from the set because it was not soluble in concentrations needed for TSA and SPR experiments. *Continues on the next page.*

Figure S6. *Continued.*
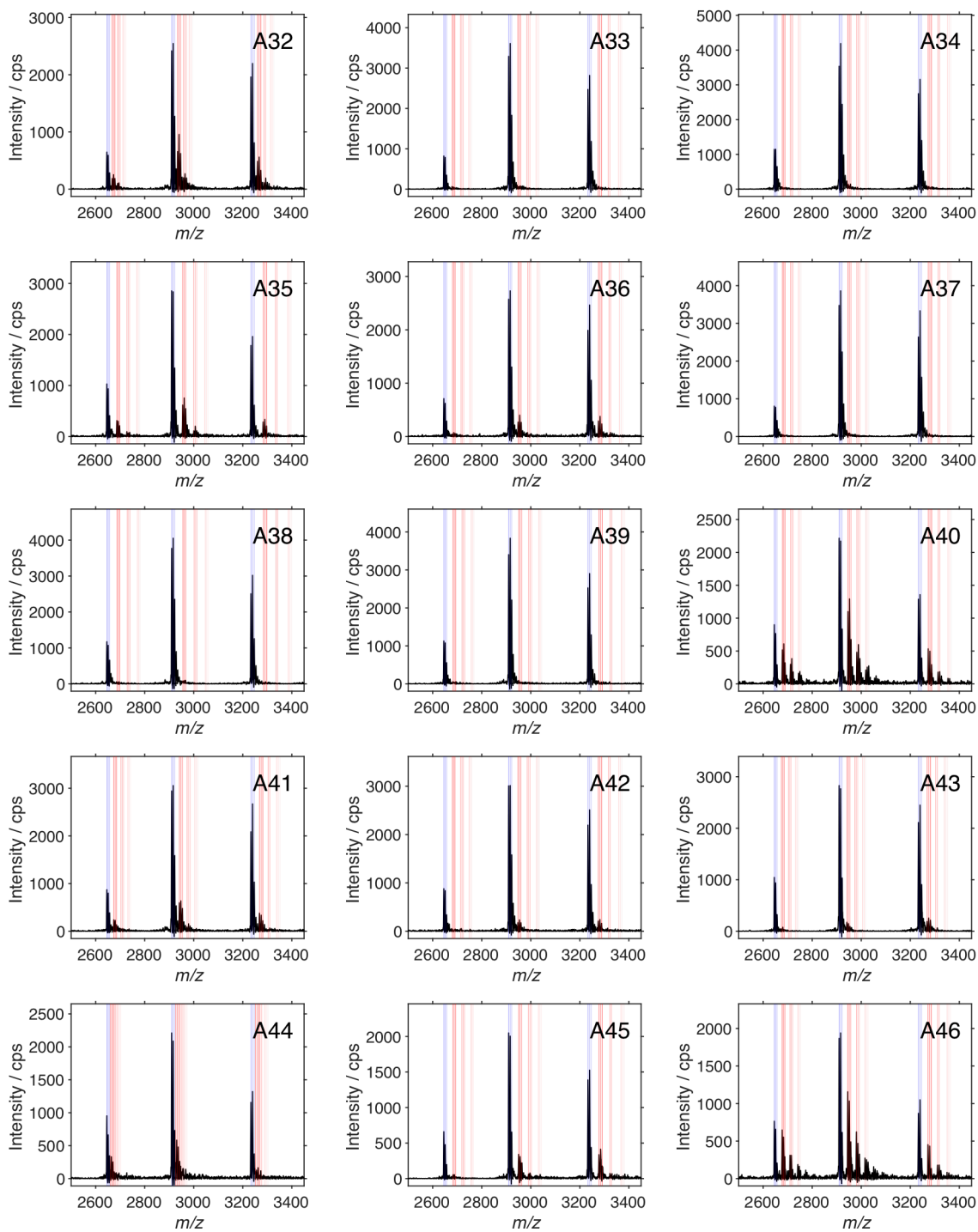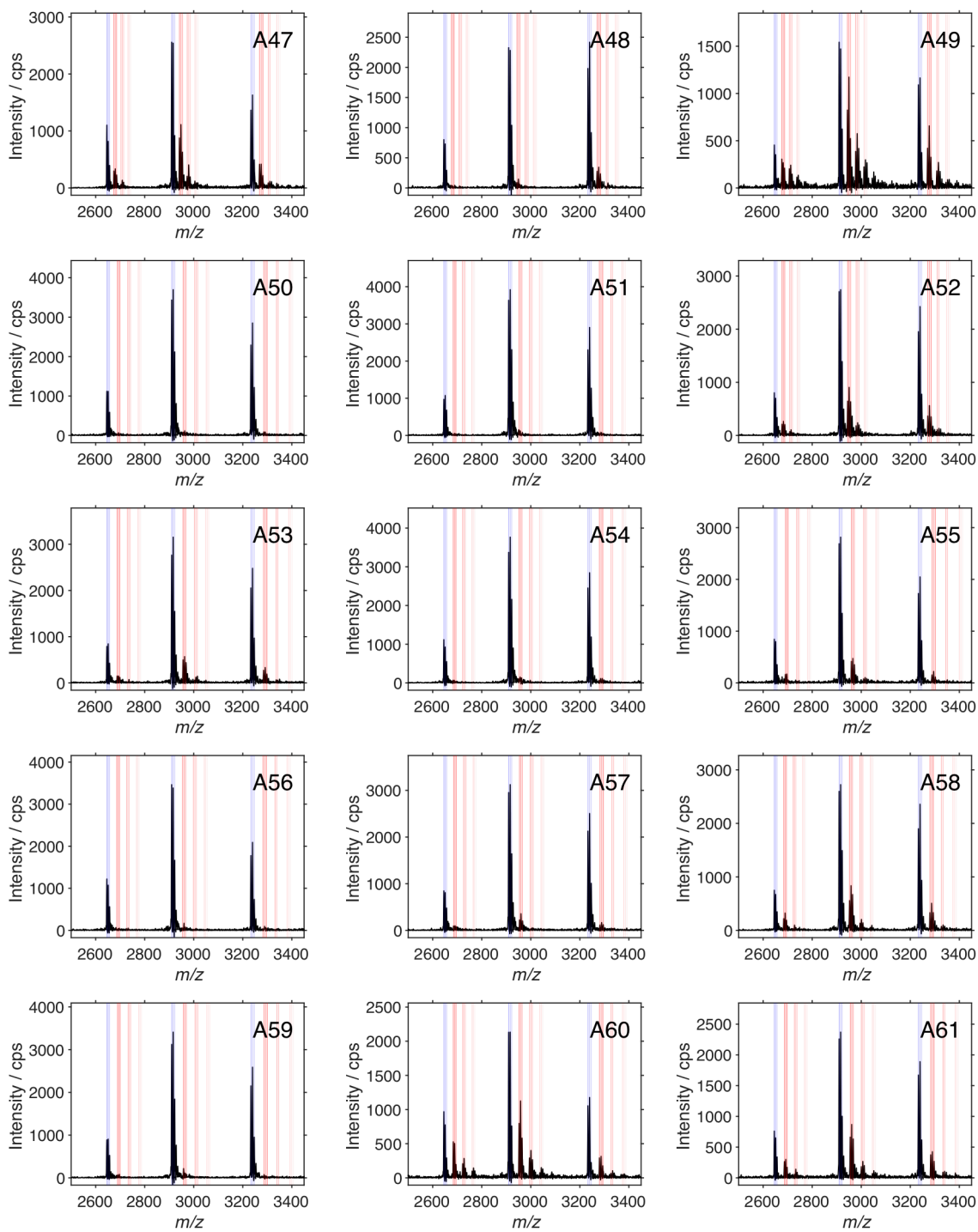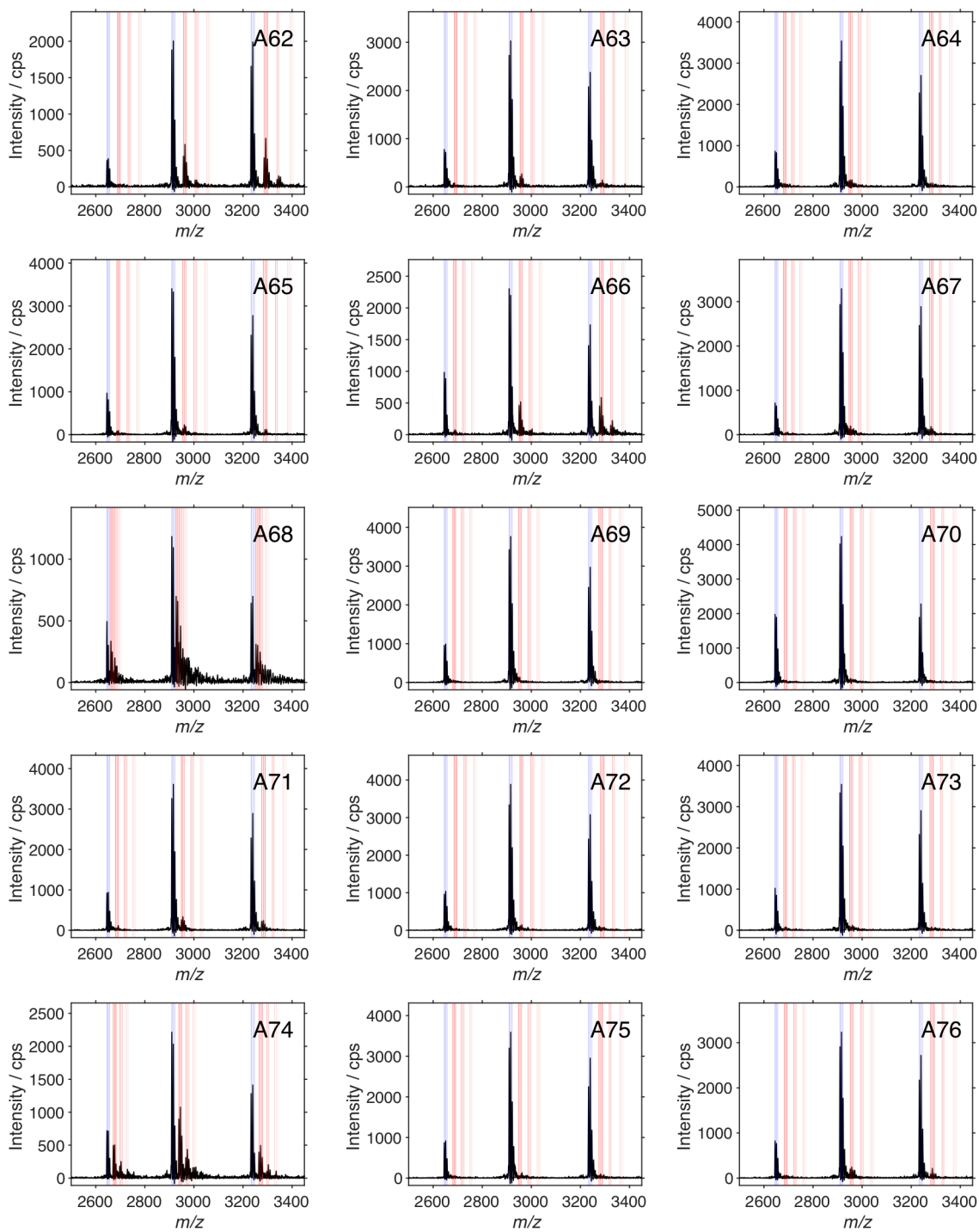
Figure S6. *Continued.*

Figure S6. *Continued.*

Figure S6. *Continued.*
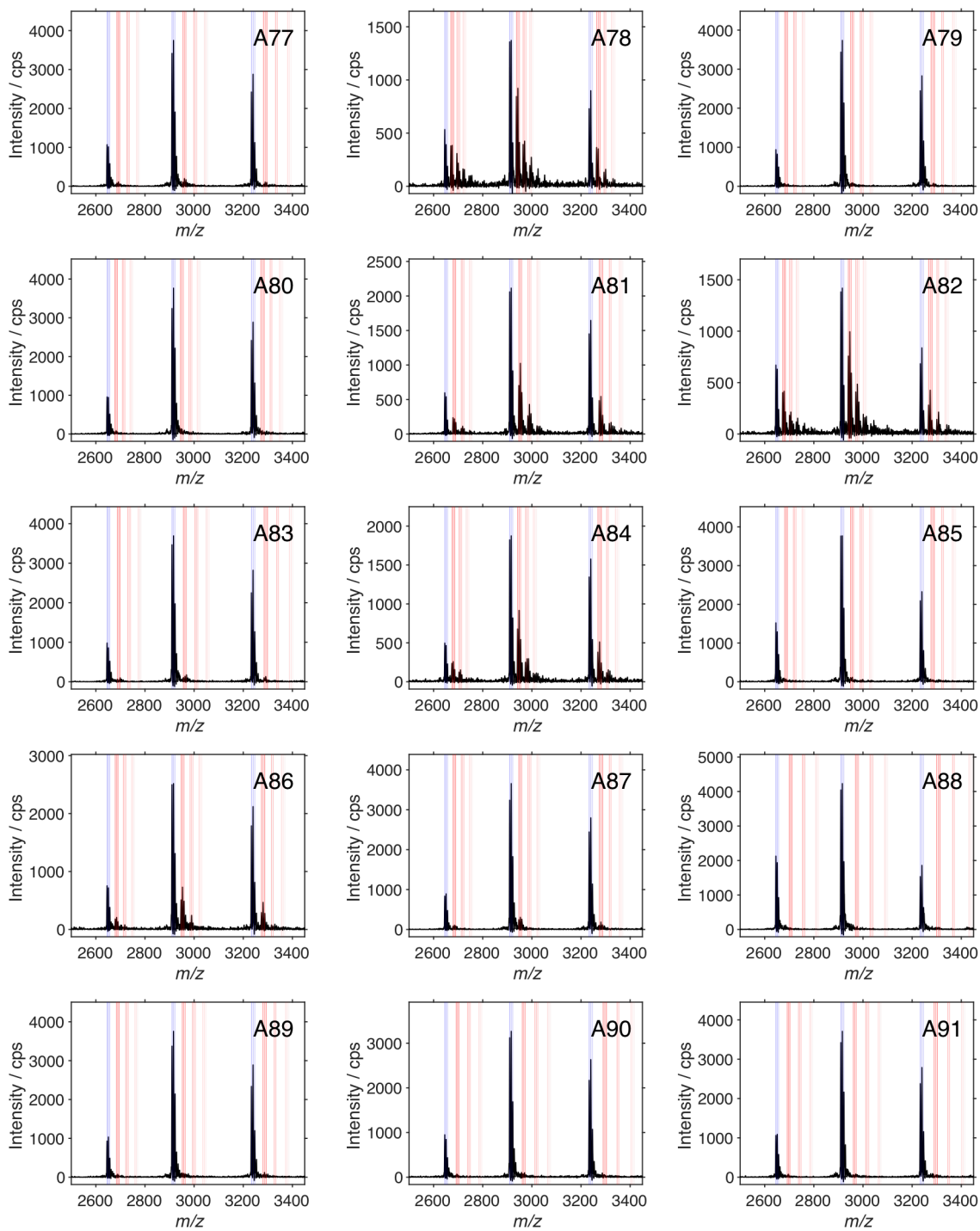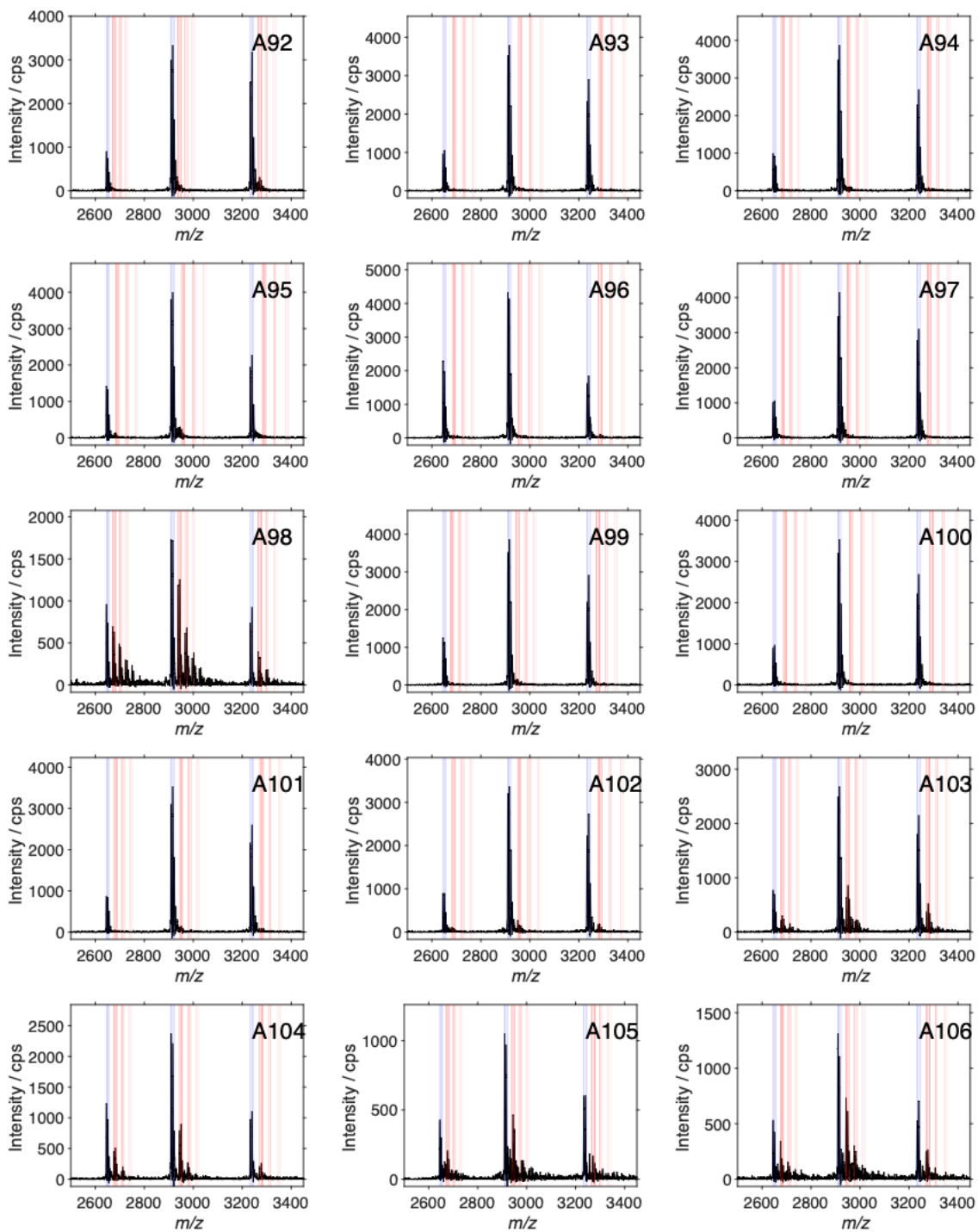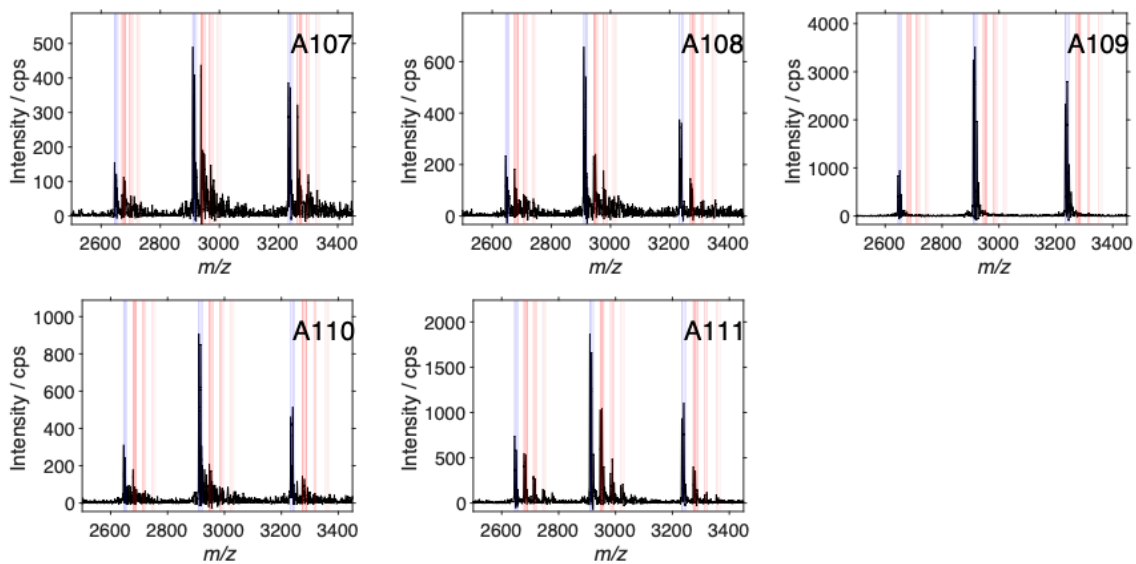
Figure S6. *Continued.*

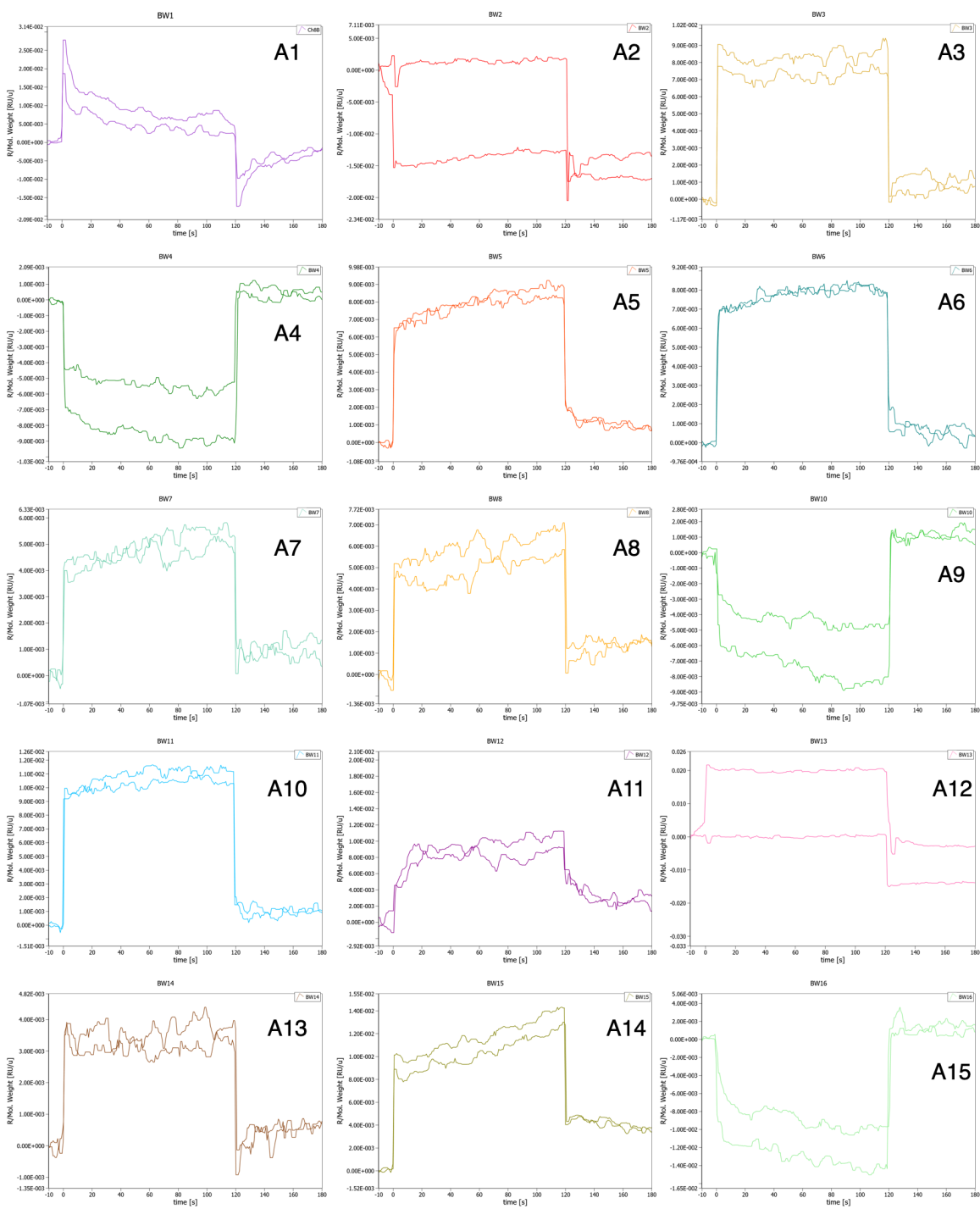Figure S6. *Continued.*

Figure S6. *Continued.*

Figure S7. Surface plasmon Resonance sensorgrams acquired for the qualitative screening of the ligands **A1** to **A111**. **A98** was not soluble at the required concentration for SPR. *Continues on the next page.*
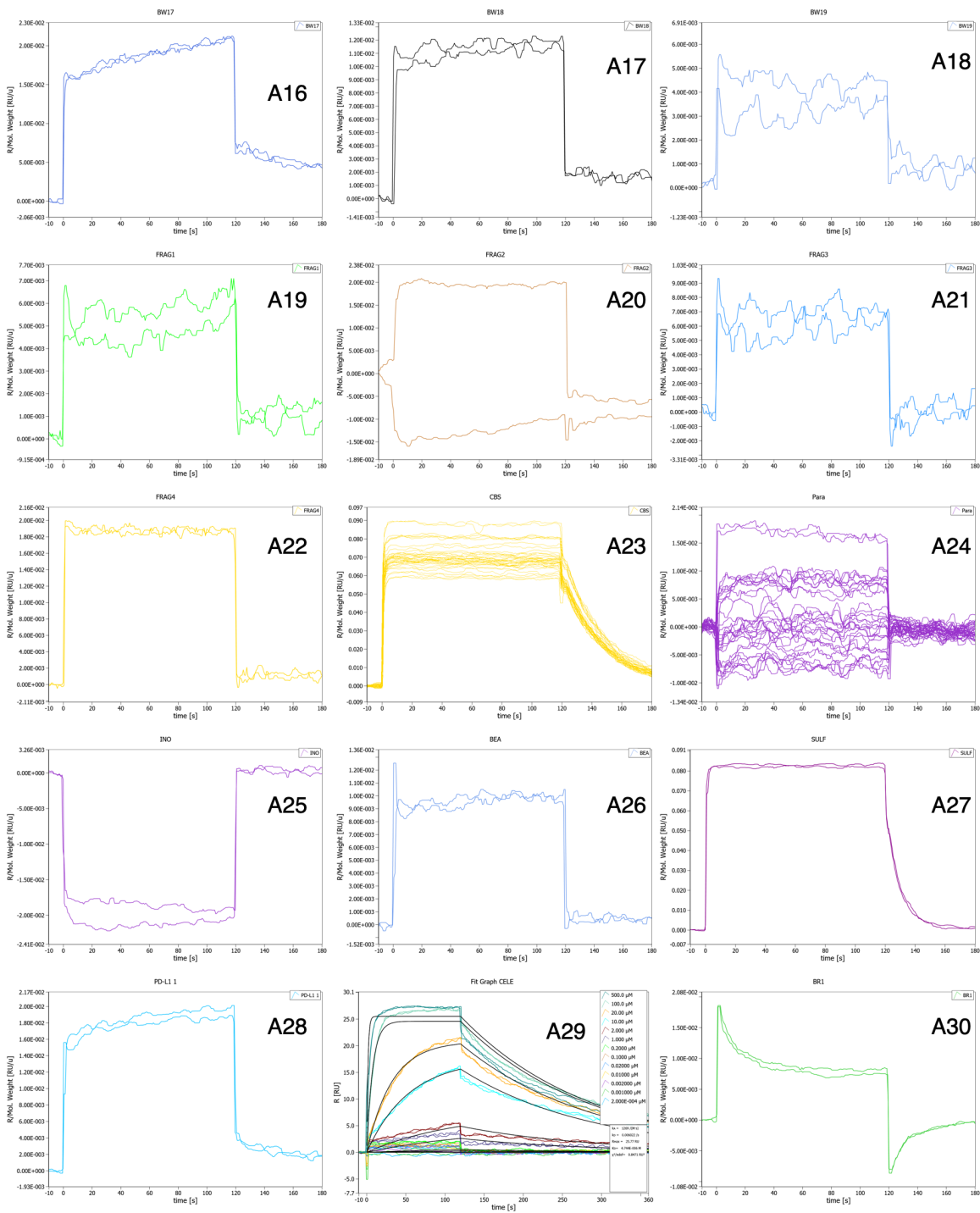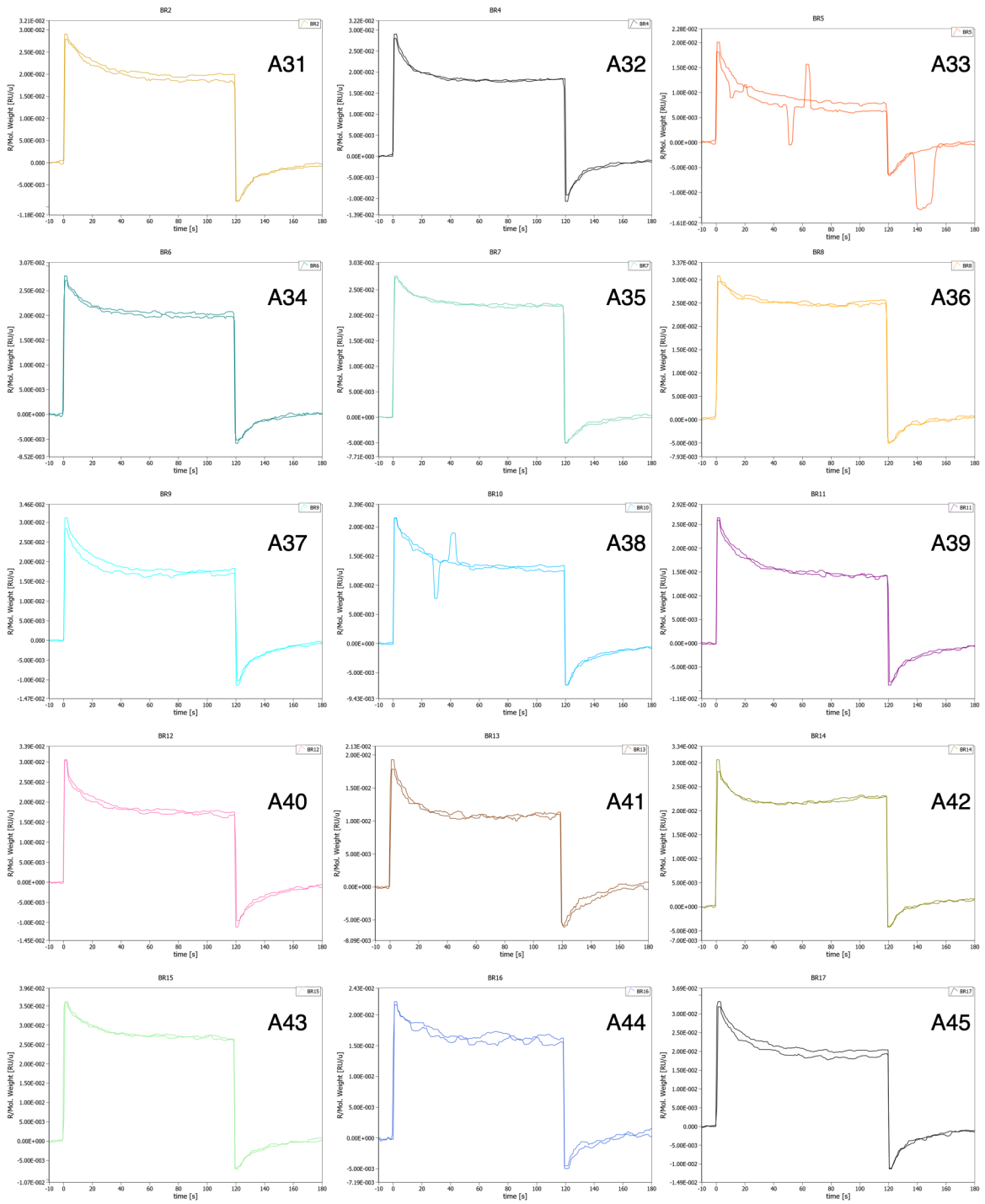
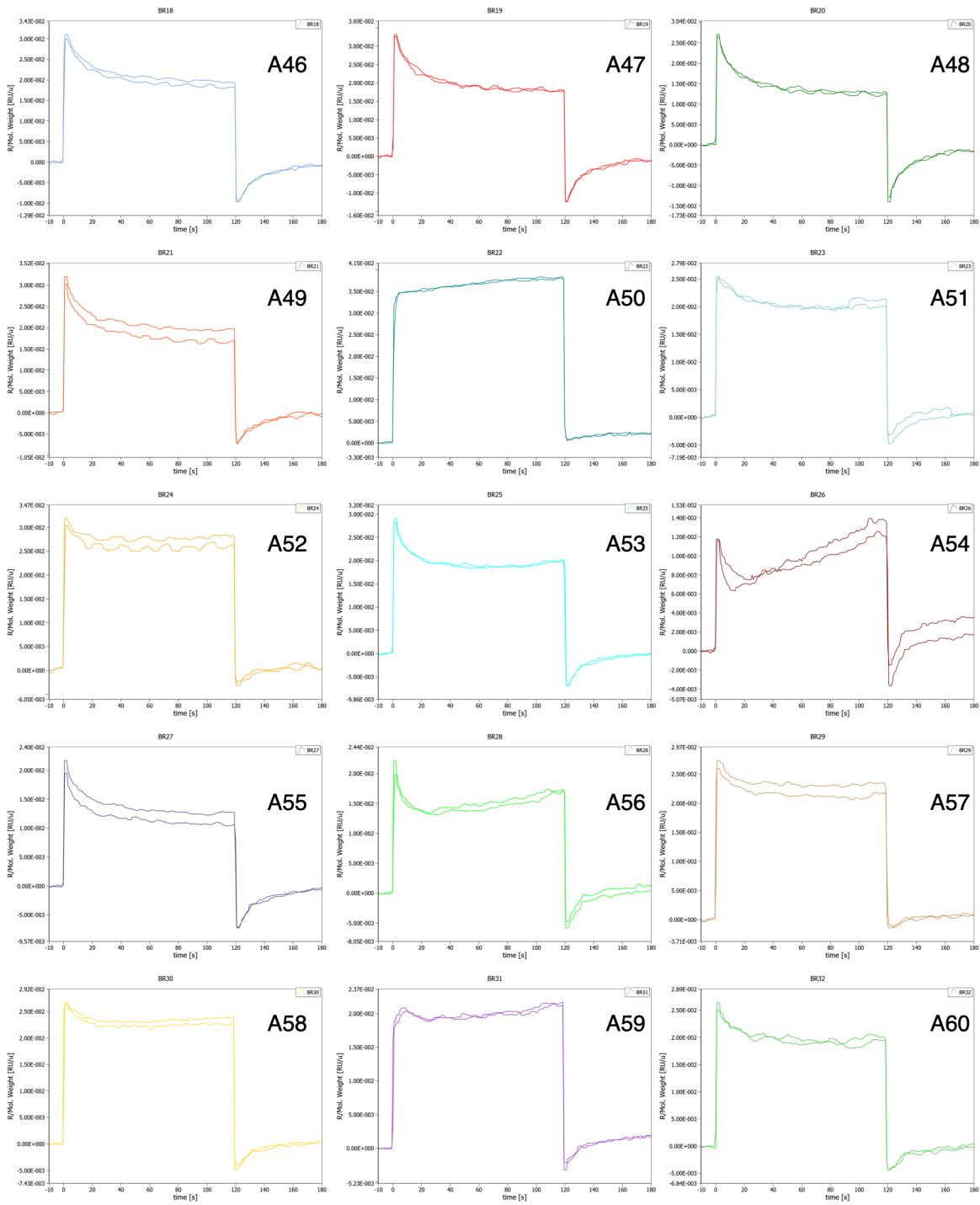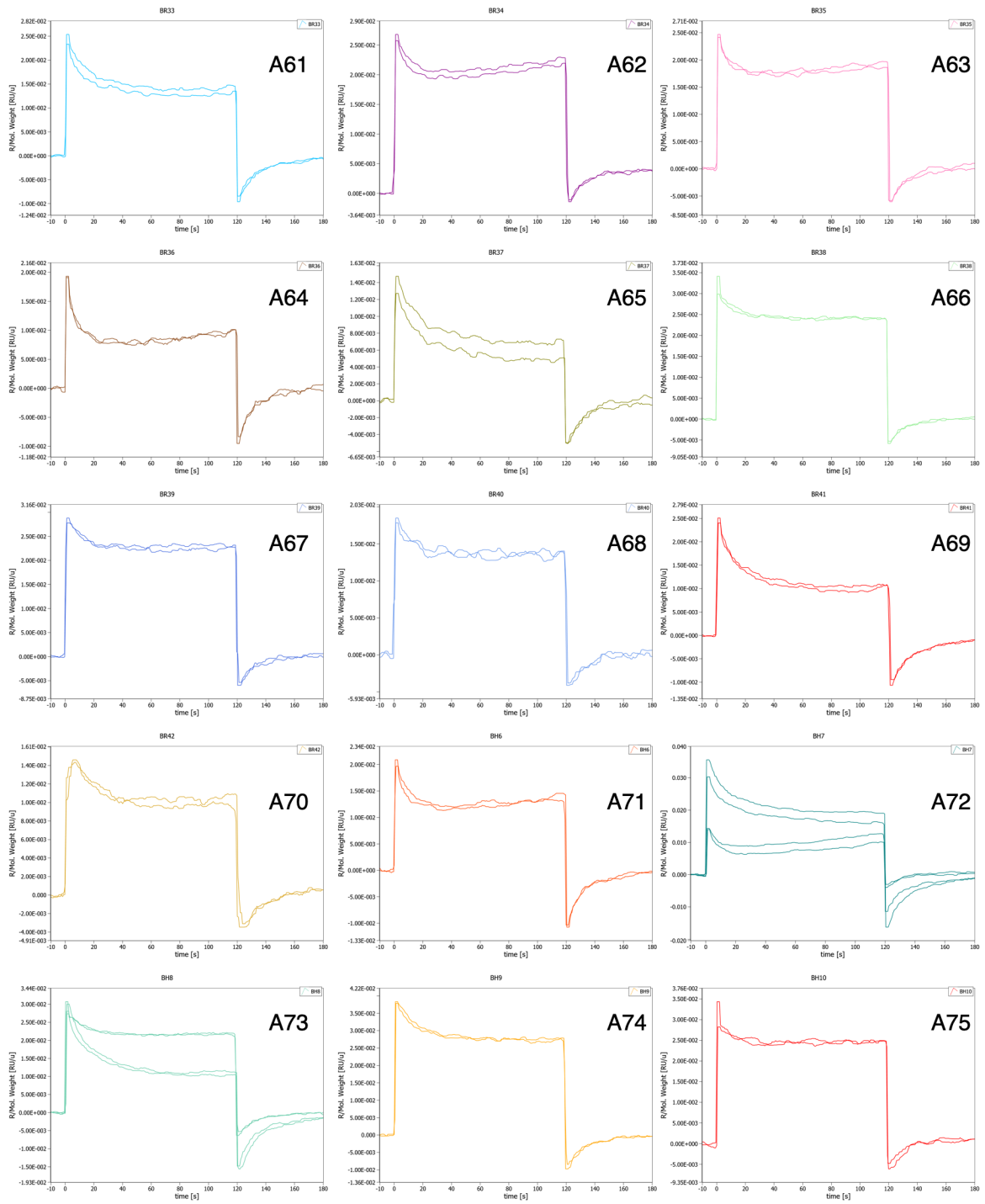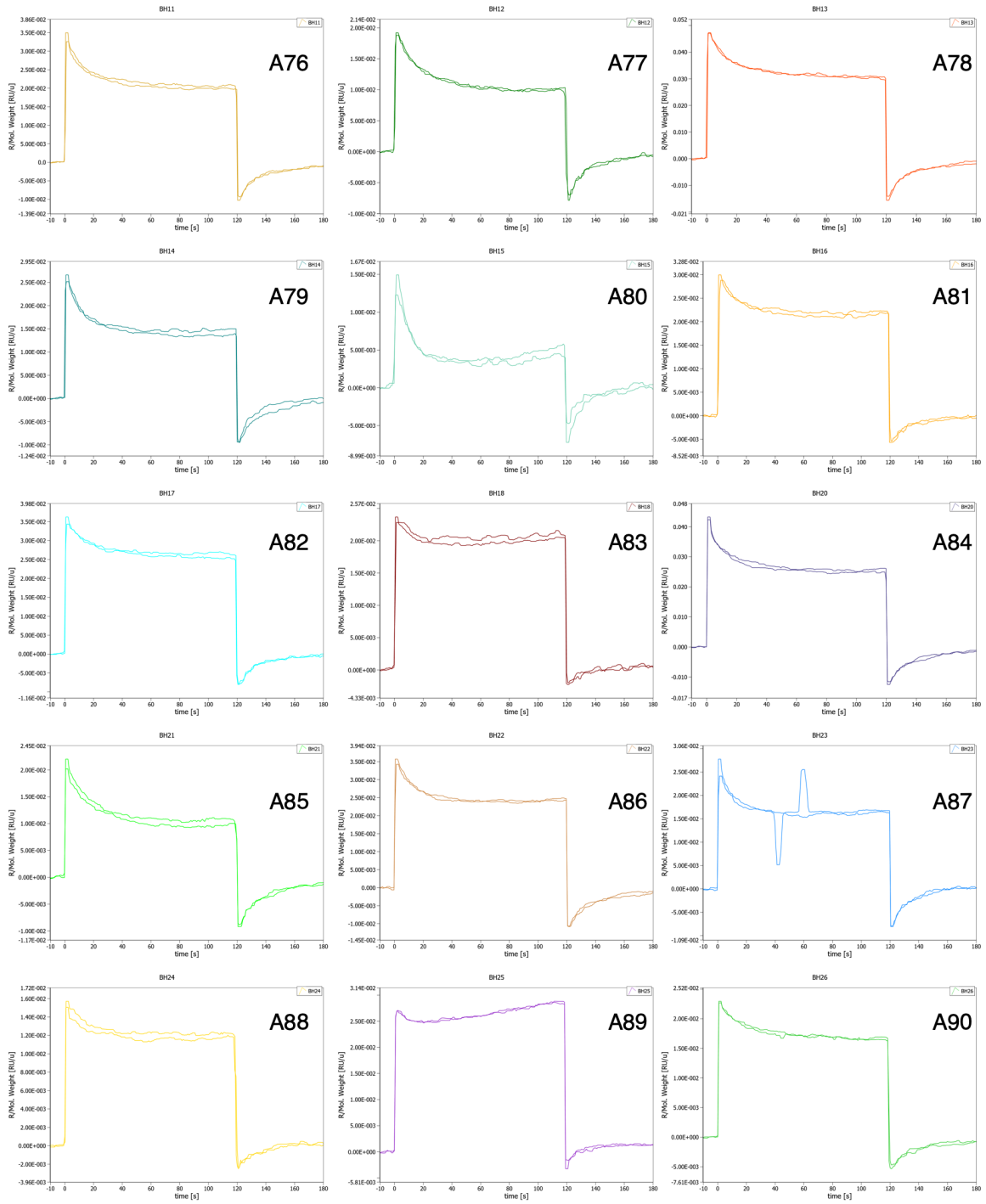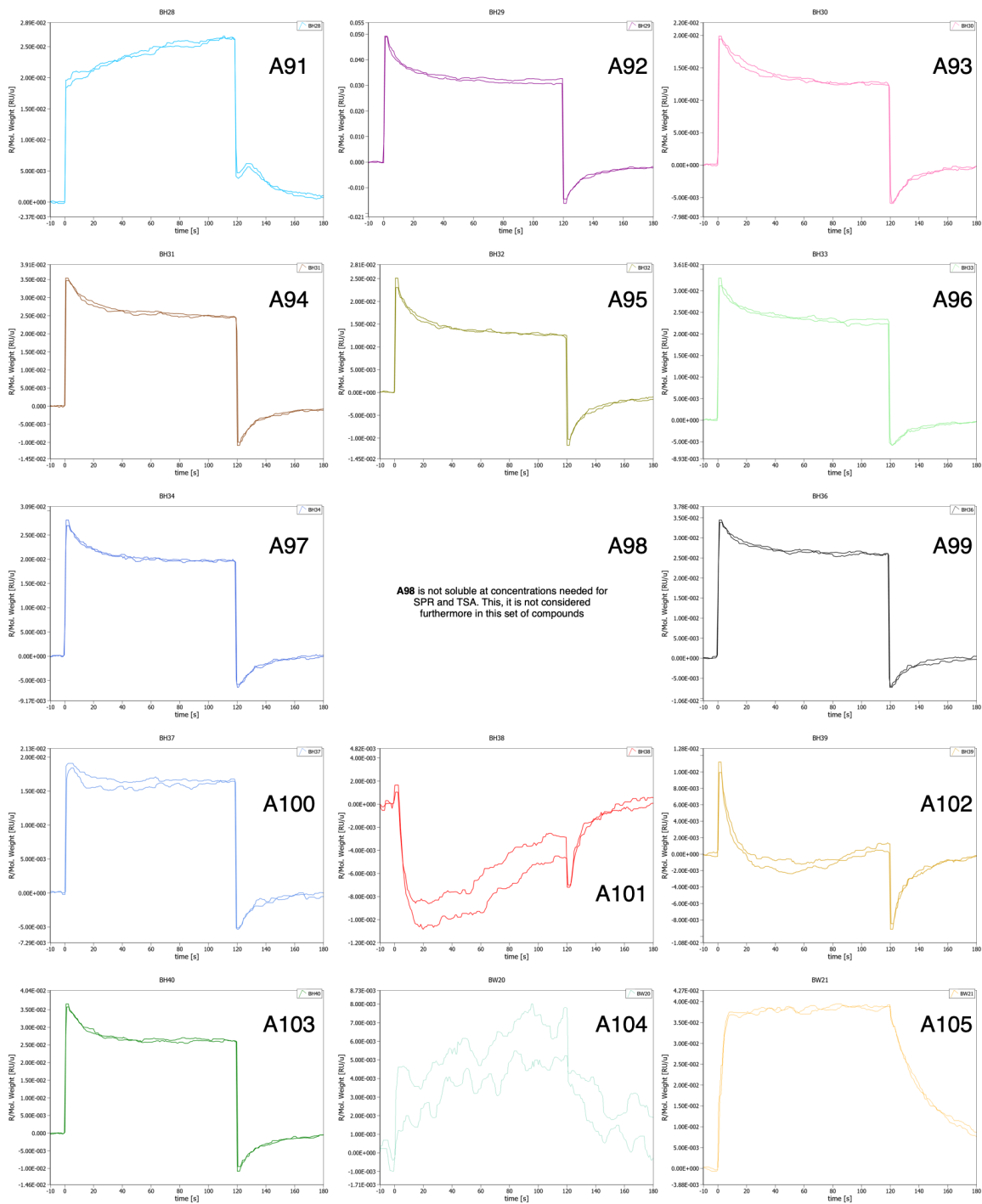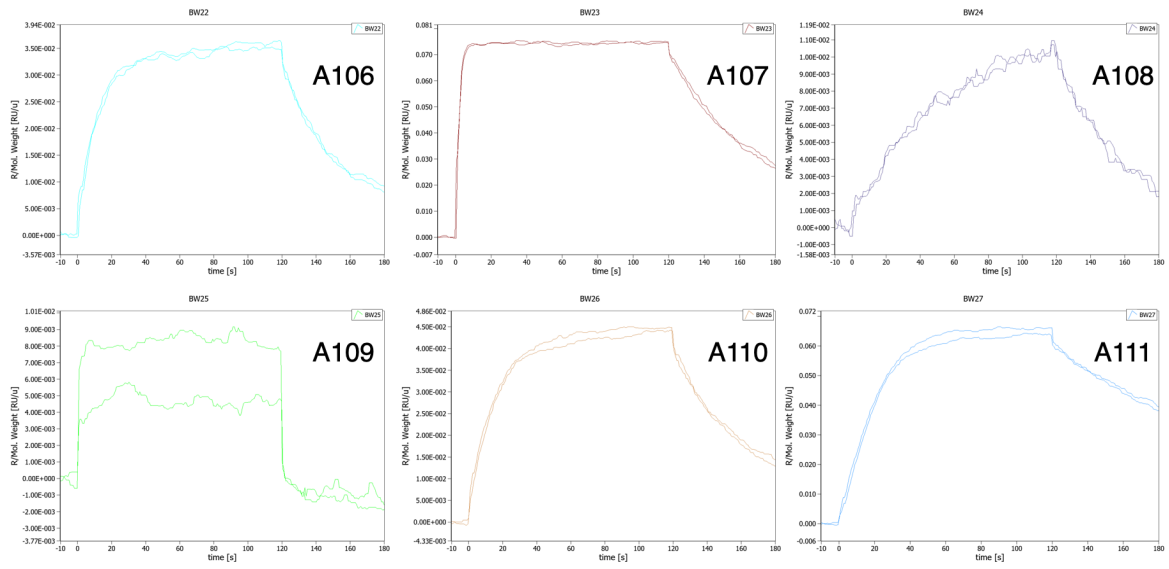Figure S7. *Continued.*

Figure S7. *Continued.*

Figure S7. *Continued.*

Figure S7. *Continued.*

Figure S7. *Continued.*

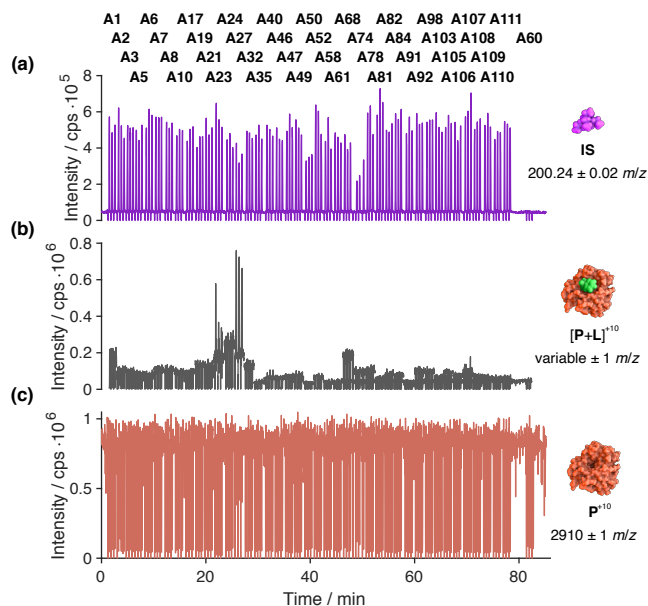Figure S7. *Continued.*

Figure S7. *Continued*.

Figure S8. Second round qualitative screening of the 41 compounds subset of the initial 111 compounds library with three repetition. Non-binding **A60** lacking the **IS** was excluded from further analysis but precipitating **A29** was included as binder. **A98** was later removed from the set because it was not soluble in concentrations needed for TSA and SPR experiments. 600 µM **L** and 600 µM **IS** are dissolved in 12:88 DMSO:buffer, expect for **A27** which was dissolved in buffer only and **A60** which lacks the **IS**. This solution is injected into a 100% buffer feed containing 5.5 µM **P** and 0.5 µM **IS**. The average injected $[\mathbf{L}]_{max}$ is estimated at 26 µM (not quantified due to ion suppression). (a) shows the XIC of the **IS** present both in the feed as well as in the injected solution. (b) The XIC at the mass, where the complex $[\mathbf{P+L}]^{+10}$ would be observed if a binder was injected. (c) shows the XIC of the unbound $\mathbf{P}^{+10}$. Upon injection of the DMSO containing **L** solution, the dominating charge state shifts from +10 to +9. This is the reason, why there is always a considerable depletion of $\mathbf{P}^{+10}$ expect for when the DMSO free binding **A27** solution is injected.
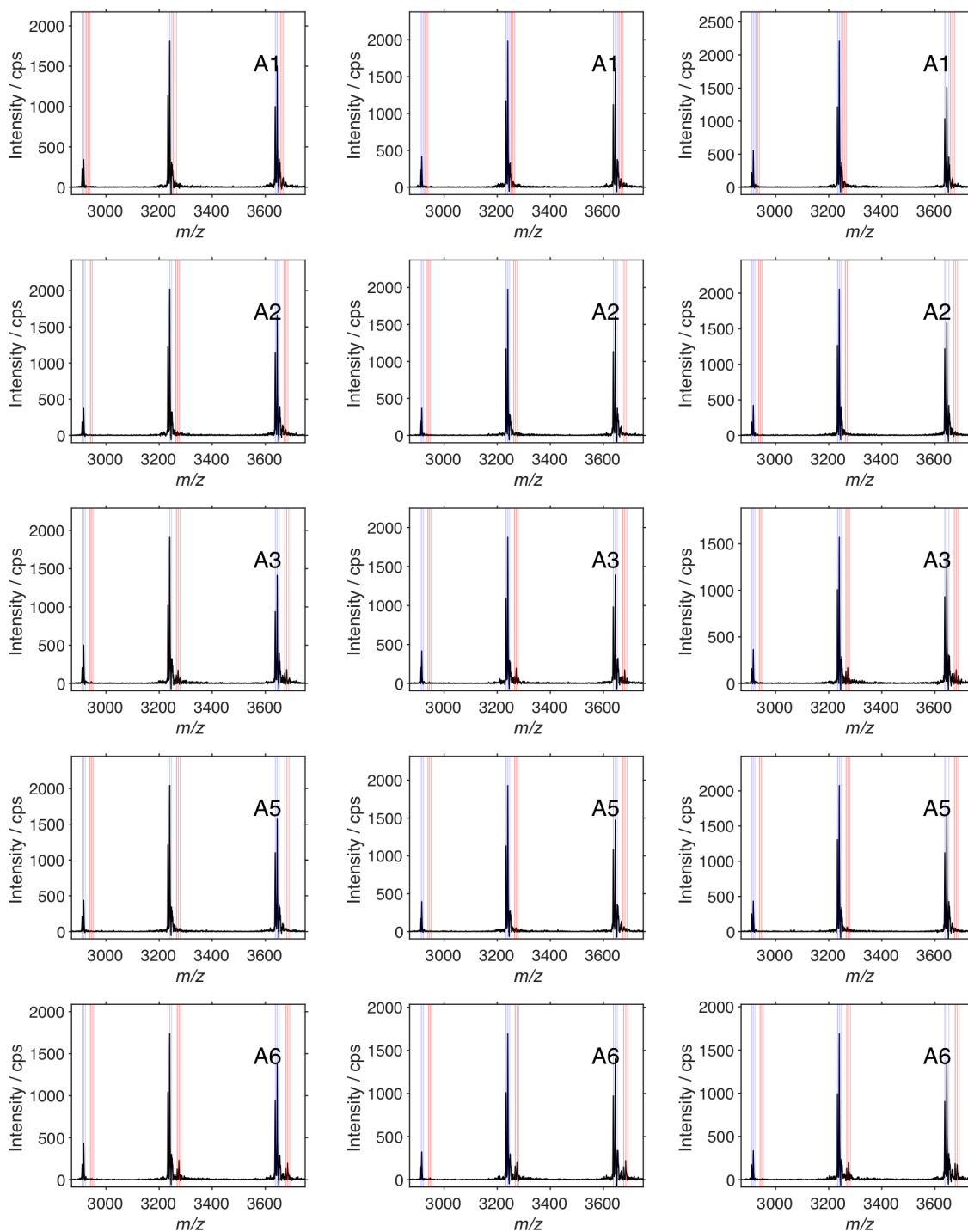
Figure S9. Mass spectra acquired for the qualitative screening of the 41 compounds subset from the 111 compound library. **A98** was later removed from the set because it was not soluble in concentrations needed for TSA and SPR experiments. The shown spectra have the highest ratio $\overline{R} = I([\mathbf{P} + \mathbf{Ac}_q + \mathbf{L}]^{+n})/I([\mathbf{P} + \mathbf{Ac}_q]^{+n})$ during one injection cycle (see figure S4), where $q=0,1,2$ are acetate adducts. Thus, the shown spectra are acquired only for 1 s. They were smoothed and baseline subtracted. The red (bound) and the blue (unbound) rectangles mark the integration limits for +10, +9 and +8 charge states of $\mathbf{P}^{+n}$, $[\mathbf{P}+\mathbf{Ac}]^{+n}$, $[\mathbf{P}+\mathbf{Ac}_2]^{+n}$, $[\mathbf{P}+\mathbf{L}]^{+n}$, $[\mathbf{P}+\mathbf{Ac}+\mathbf{L}]^{+n}$, $[\mathbf{P}+\mathbf{Ac}_2+\mathbf{L}]^{+n}$, which are used to determine the K_D value. The charge state is different here, because upon injection of the DMSO solution into the buffered **P** solution, the charge state shifts. *Continues on the next page.*

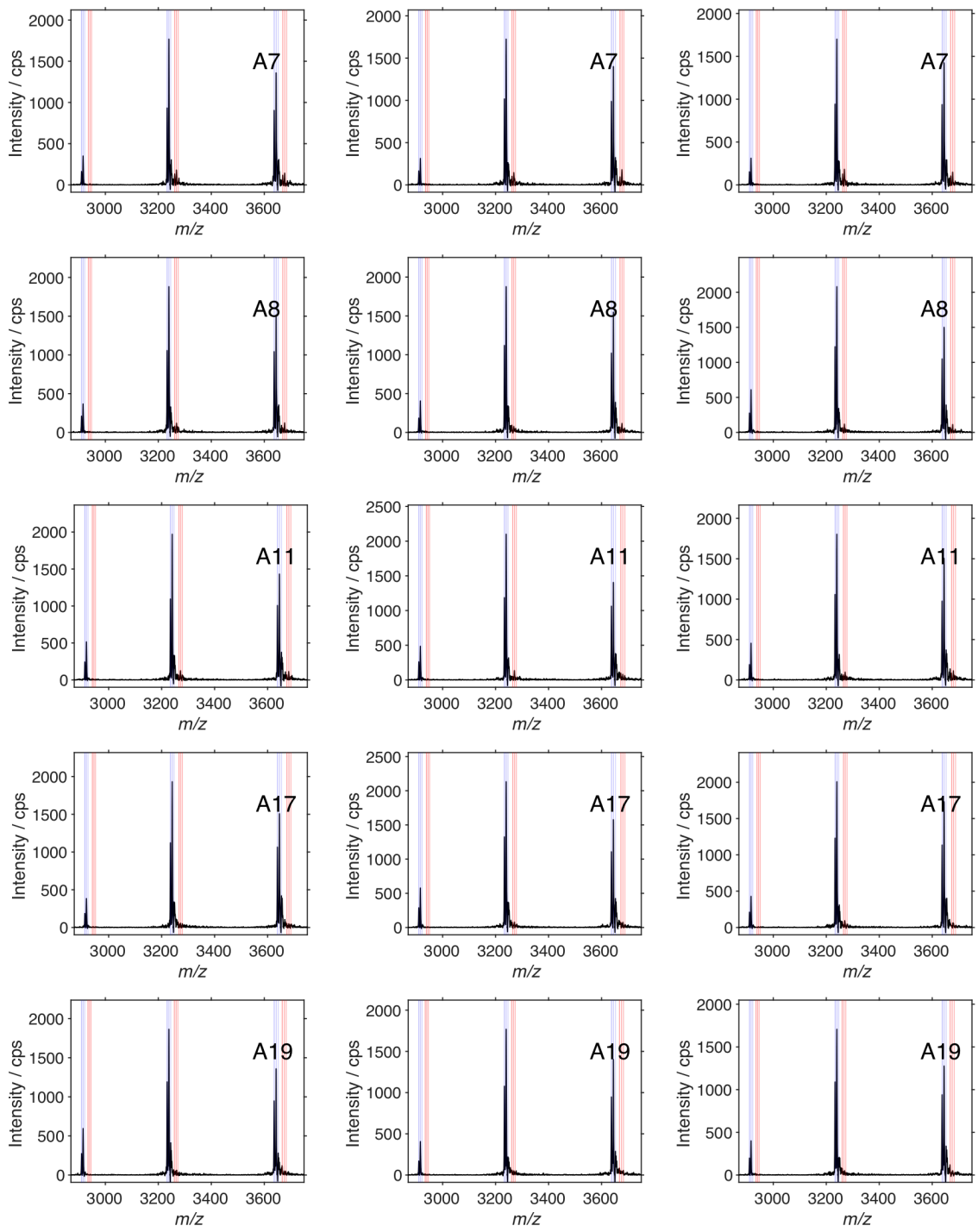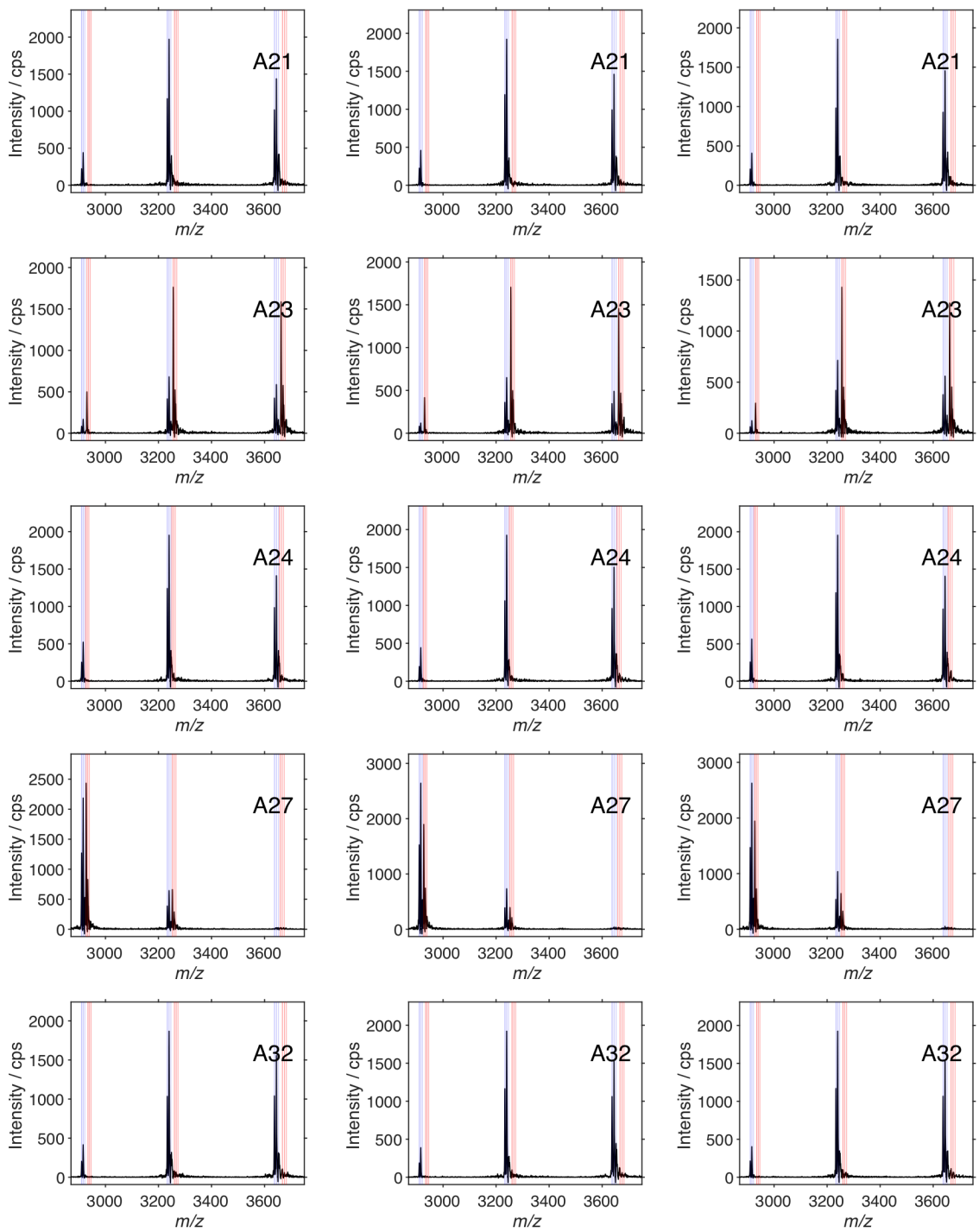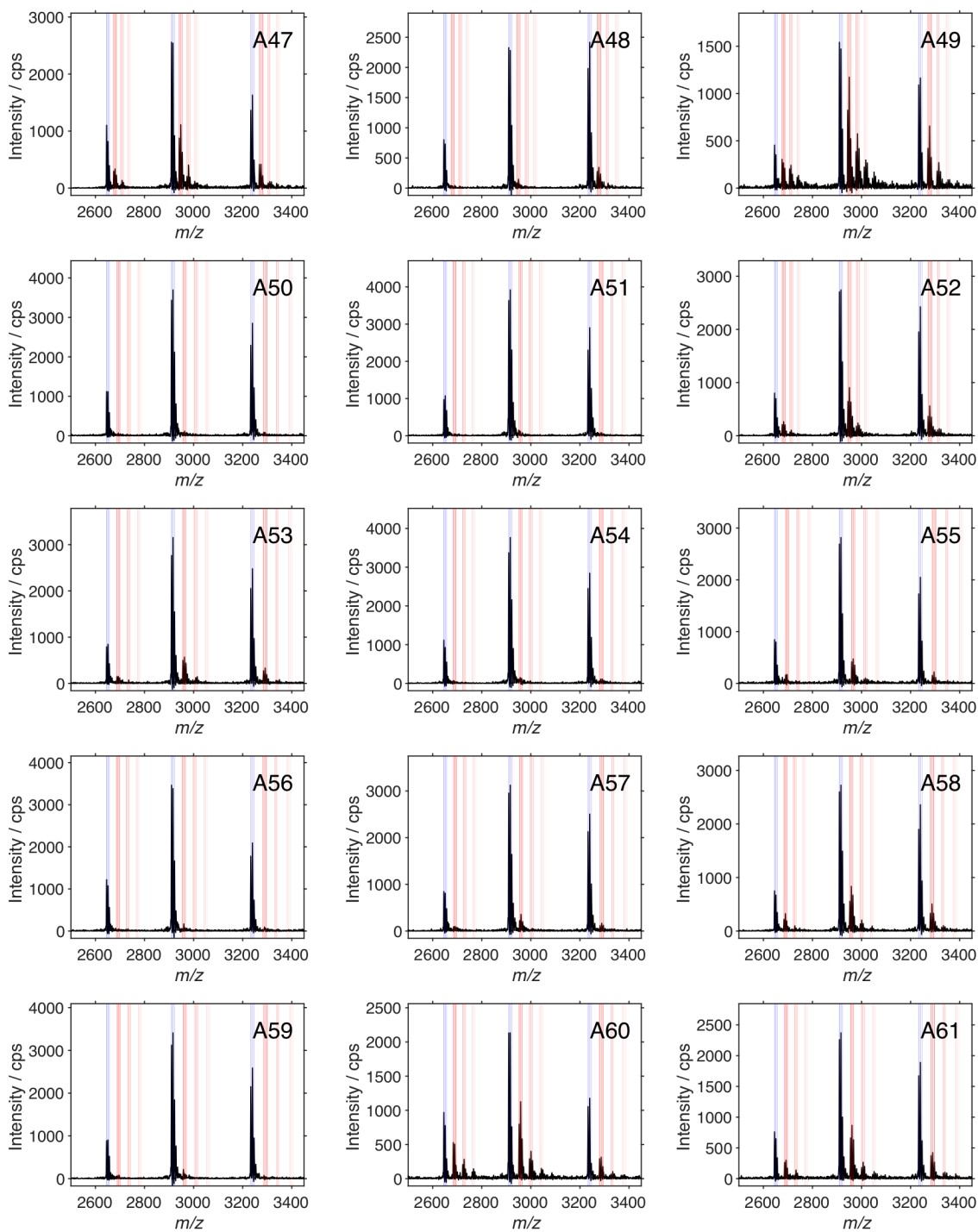Figure S9. *Continued.*
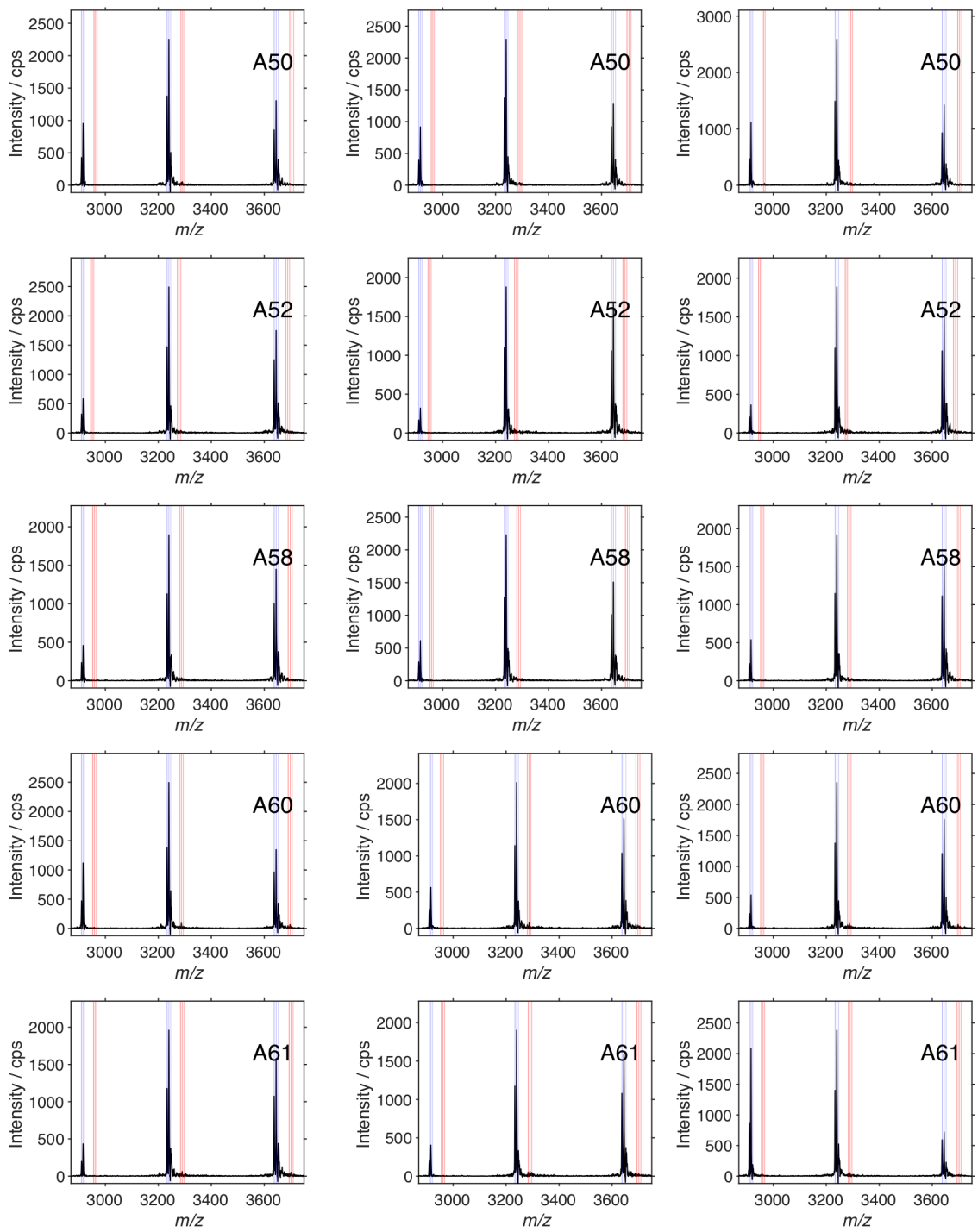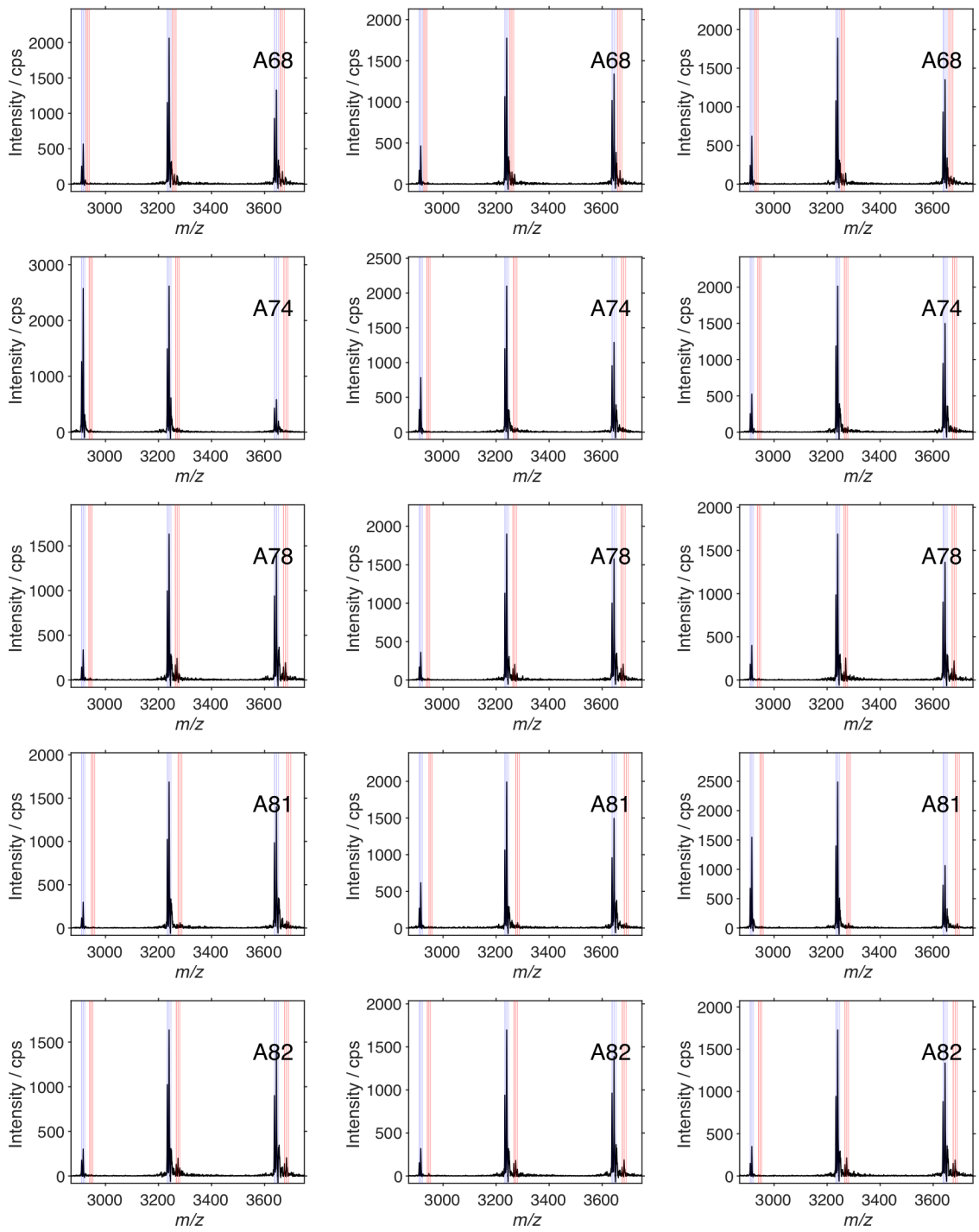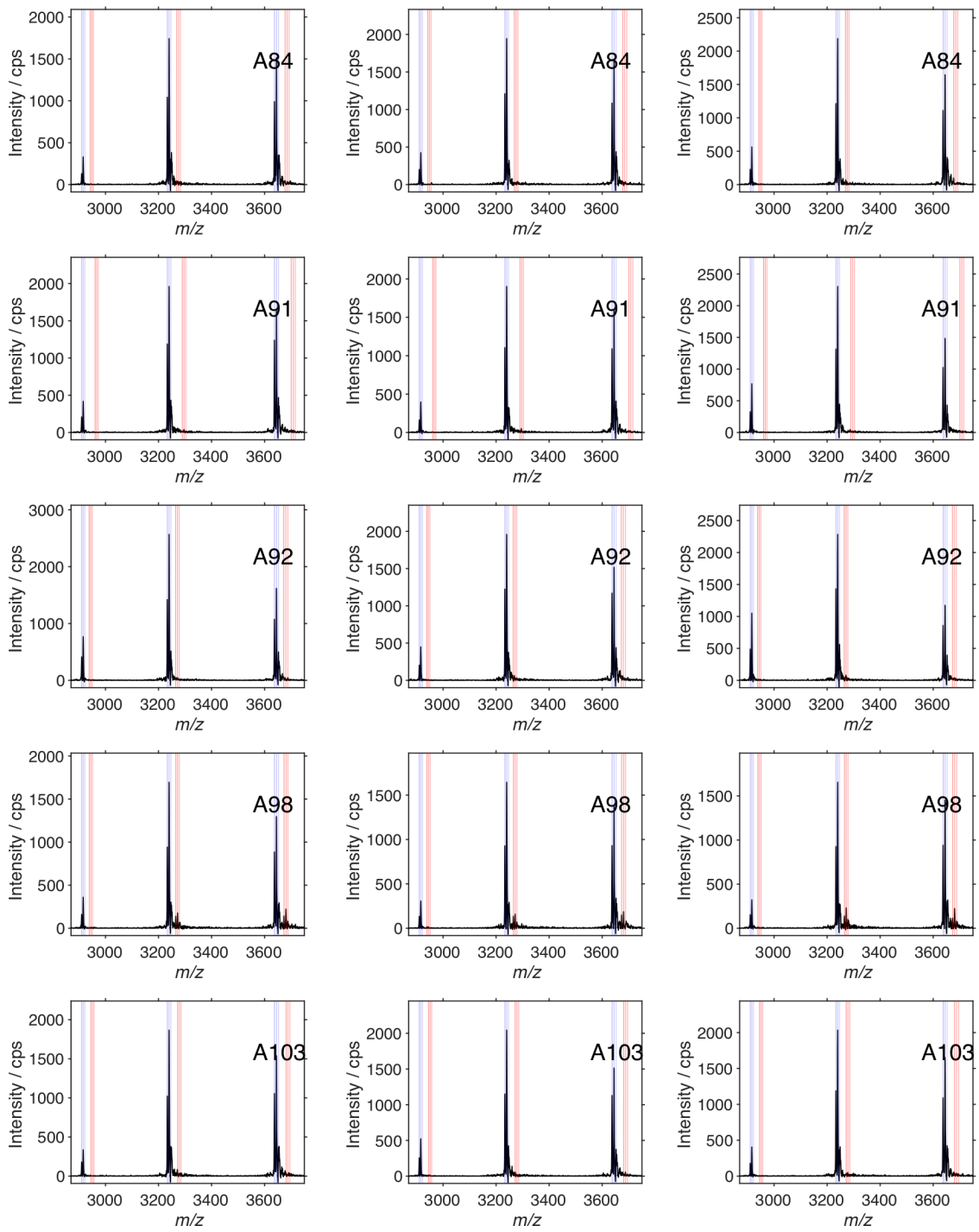
Figure S9. *Continued.*

Figure S9. *Continued.*

Figure S9. *Continued.*

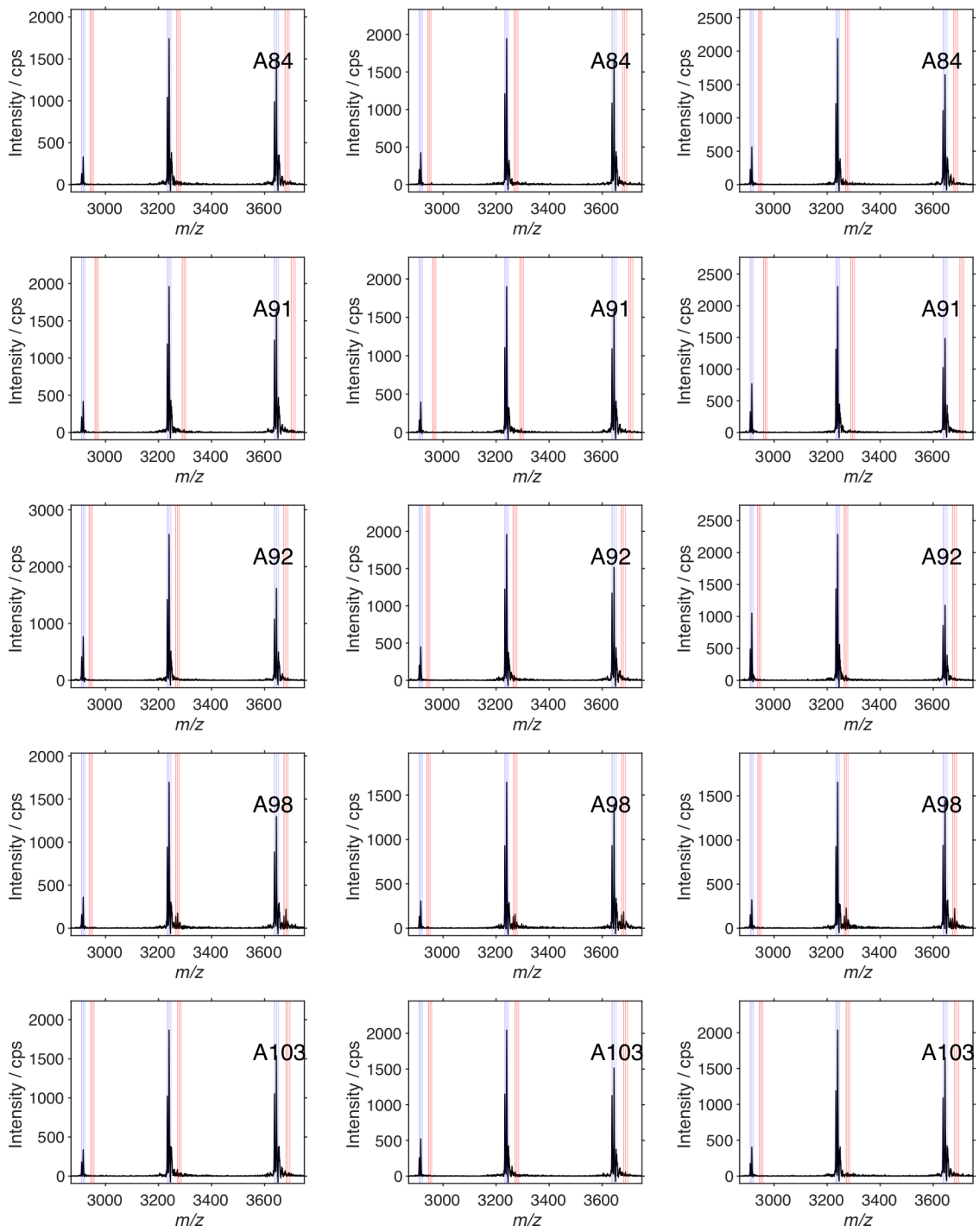Figure S9. *Continued.*

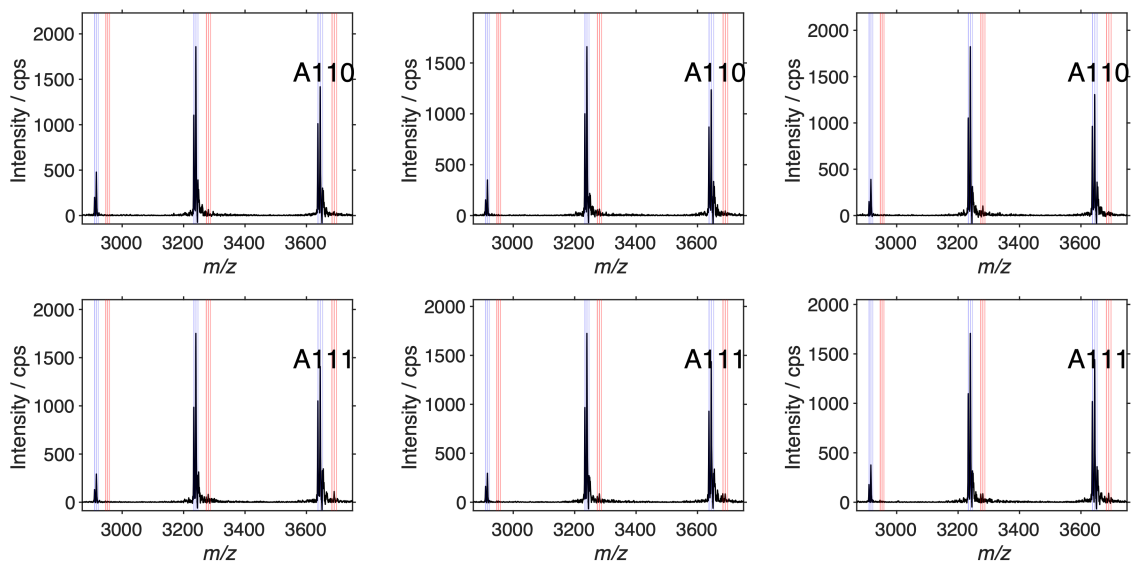Figure S9. *Continued.*
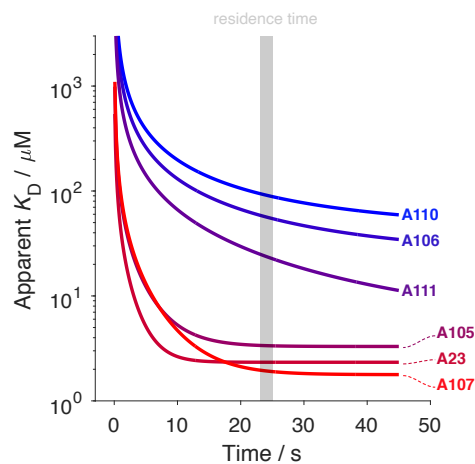
Figure S9. *Continued.*

Figure S9. *Continued.*

Figure S10. Binding kinetic modelling for some slow binding ligands used for the second round of qualitative screening. The kinetic constants k_{on} and k_{off} were determined by SPR (see table S1). Upon injection of **L** into the **P** feed, the formation of the complex **[P+L]** should proceed according to the following differential equation:

$$\frac{d[\mathbf{P+L}]}{dt} = k_{on}[\mathbf{L}][\mathbf{P}] - k_{off}[\mathbf{P+L}]$$
$$= k_{on}([\mathbf{L}]_{tot} - [\mathbf{P+L}])([\mathbf{P}]_0 - [\mathbf{P+L}]) - k_{off}[\mathbf{P+L}]$$

Where **[P+L]** is the complex concentration, **[L]** the free ligand concentration, **[P]** the free protein concentration, $[\mathbf{L}]_{tot}$ the total ligand concentration and $[\mathbf{P}]_0$ the total protein concentration fed into the open capillary. The boundary condition is

$$[\mathbf{P+L}](0) = 0$$

i.e., at the timepoint 0 after injection, there is no complex formed yet. Using the dsolve function of Matlab R2018a an analytical solution can be found for the differential equation. For the modelling, the actual **P** feed concentration $[\mathbf{P}]_0 = 5.5\,\mu M$ is used. The average injected maximum concentration is $[\mathbf{L}]_{max} = 25\,\mu M$, thus $[\mathbf{L}]_{tot} = 25\,\mu M$ is chosen. The solution function is then fed with time points from 1 to 45 s. This yields in $[\mathbf{P+L}](t)$ at every timepoint t. The free protein concentration can be computed by $[\mathbf{P}](t) = [\mathbf{P}]_0 - [\mathbf{P+L}](t)$. Therefore, the apparent $K_D(t)$ can be calculated at t. The apparent $K_D(t)$ does not represent the equilibrium but instead the ratio of the species on their way towards equilibrium. Thus, it represents the misinterpretation of the dissociation constant K_D by reading out the species ratio before they reached equilibrium. In the shown experiment, the residence time was 24 s (grey rectangle). In particular, **A110** and **A106** are do not reach equilibrium within this time scale and are far from forming significant **[P+L]** species, i.e., they might be interpreted as nonbinders.
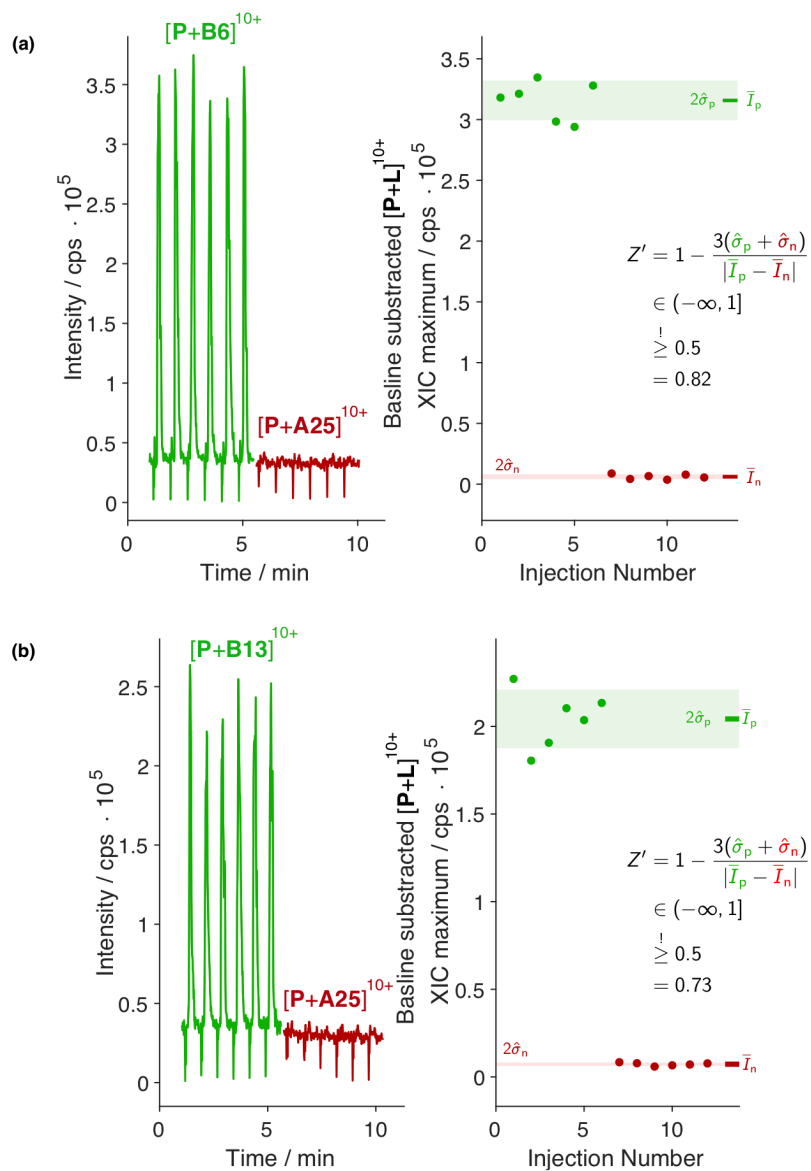
Figure S11. Z' factor for the protein complex signal $[\mathbf{P+L}]^{+10}$. In the shown experiments, 4 µM $\mathbf{P}$ and 0.5 µM $\mathbf{IS}$ are delivered at $3\,\mu l\,min^{-1}$. 600 µM $\mathbf{L}$ and 600 µM $\mathbf{IS}$ are injected into the feed. (a) $\mathbf{B6}$ is injected six times followed by six $\mathbf{A25}$ injections. Shown is the XIC of $[\mathbf{P+B6}]^{+10}$ and $[\mathbf{P+A25}]^{+10}$. On the right side of the figure, the baseline subtracted XIC maxima are shown. For the set of binding and nonbinding points, the standard deviation $\hat{\sigma}_i$ and the mean value $\bar{I}_i$ are shown. From these values, the Z' factor is calculated according to the formula in the figure.[2] $Z' = 0.82 \geq 0.5$ qualifies the screening as an excellent screening. (b) shows the same for $\mathbf{B13}$ and $\mathbf{A25}$. In this case, $Z' = 0.73$.
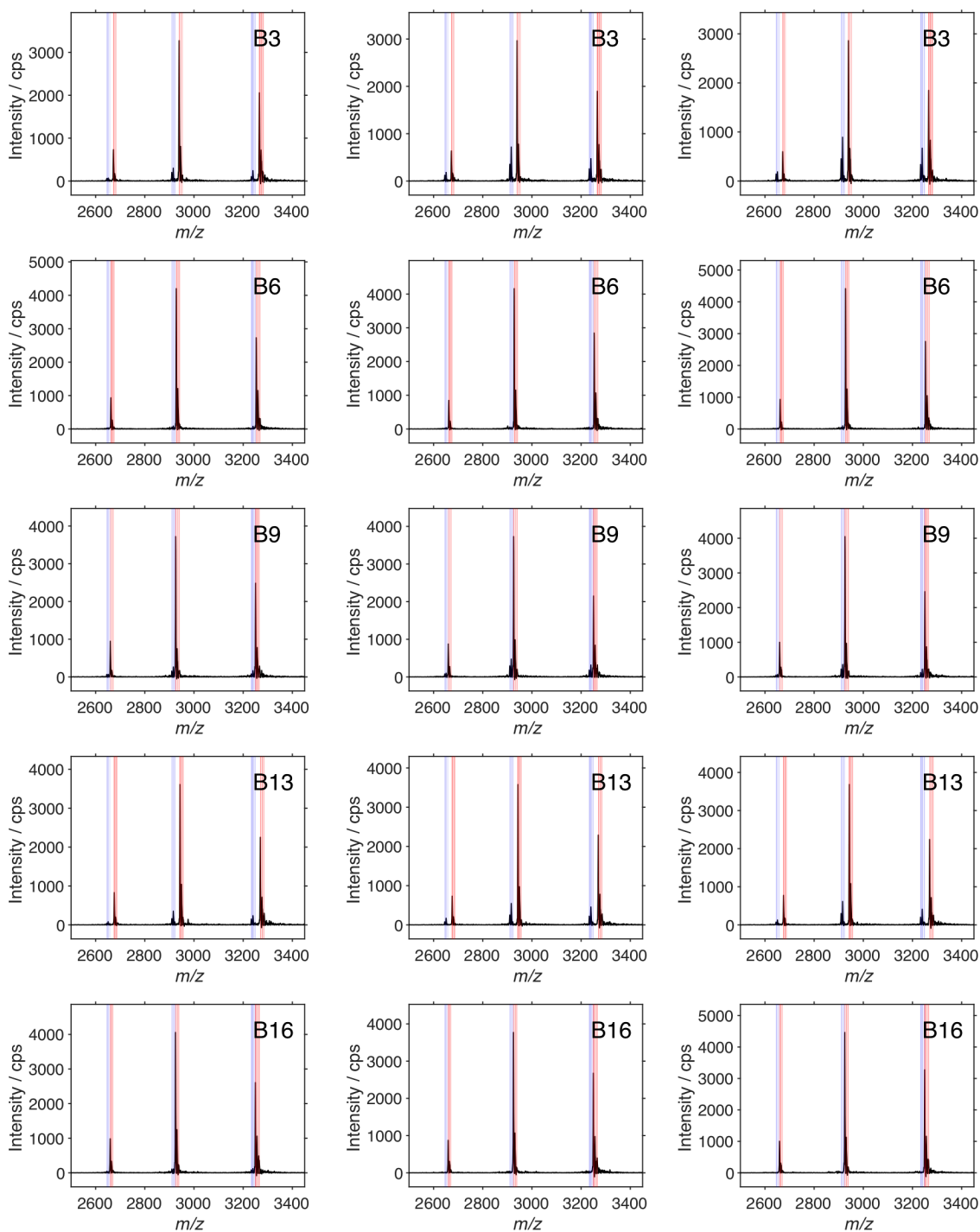
Figure S12. Mass spectra acquired for the semi-quantification of the binding ligands of the set **A23** to **A27** and **B1** to **B28**. The shown spectra have the highest ratio $\overline{R} = \overline{I([\mathbf{P} + \mathbf{Ac}_q + \mathbf{L}]^{n+})/I([\mathbf{P} + \mathbf{Ac}_q]^{n+})}$ during one injection cycle (see figure S4), where q=0,1,2 are acetate adducts. Thus, the shown spectra were acquired only for 1 s. They were smoothed and baseline subtracted. The red (bound) and the blue (unbound) rectangles mark the integration limits for 11+, 10+ and 9+ charge states of $\mathbf{P}^{n+}$, $[\mathbf{P}+\mathbf{Ac}]^{n+}$, $[\mathbf{P}+\mathbf{Ac}_2]^{n+}$, $[\mathbf{P}+\mathbf{L}]^{n+}$, $[\mathbf{P}+\mathbf{Ac}+\mathbf{L}]^{n+}$ and $[\mathbf{P}+\mathbf{Ac}_2+\mathbf{L}]^{n+}$, which are used to determine the K_D value. *Continues on the next page.*
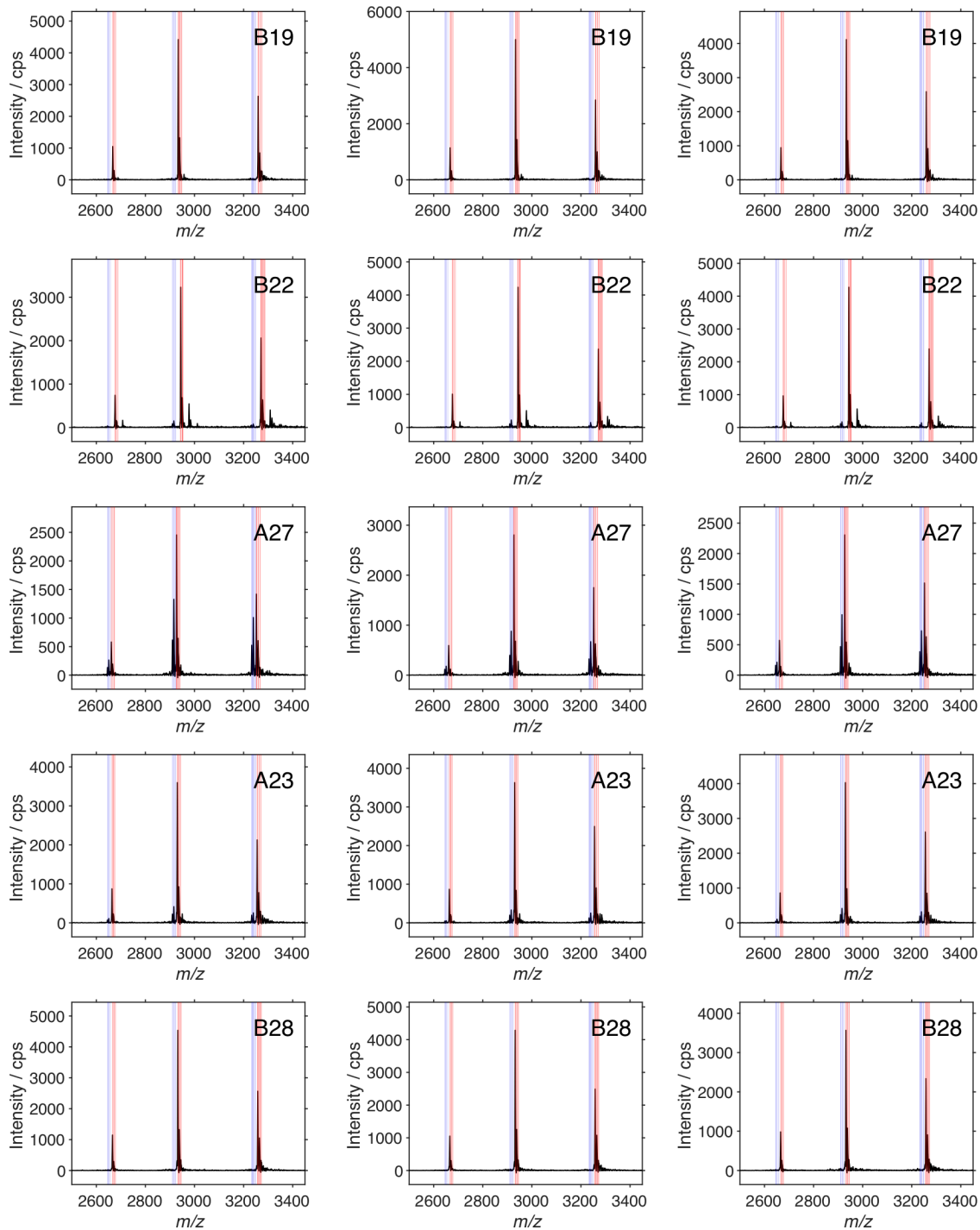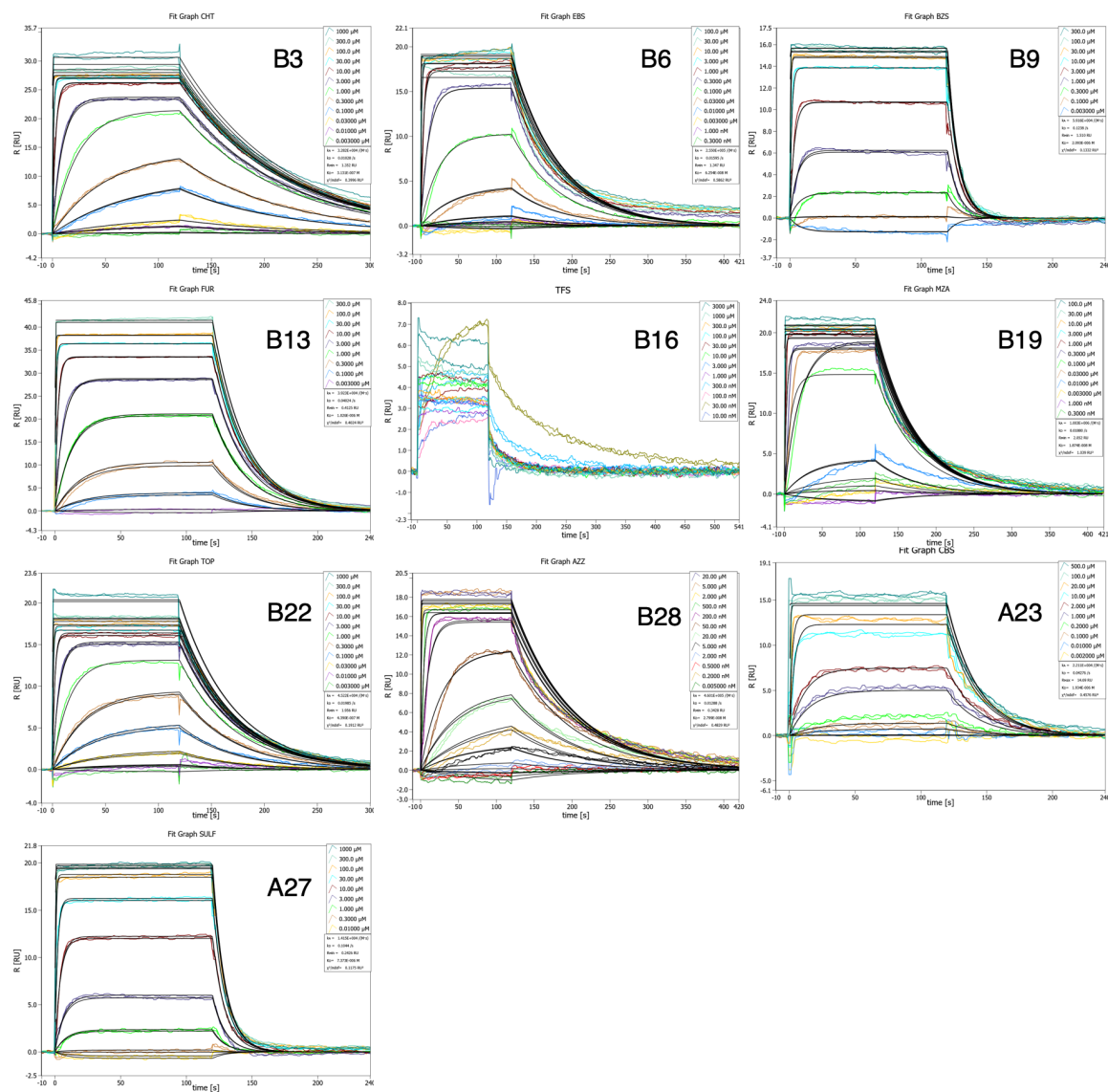
Figure S12. *Continued.*

Figure S13. Surface plasmon resonance sensorgrams acquired for the binding strength quantification of ligands **A23** and **A27** as well as the sulfonamide bearing ligands in the set **B1** to **B28**.
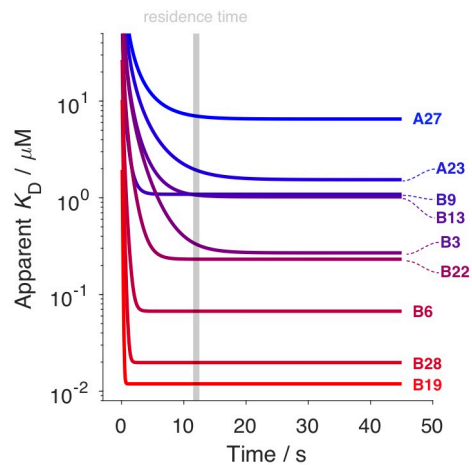
Figure S14. Binding kinetic modelling for the binding ligands used for the semi-quantification. The same model as in figure S10 was used. The kinetic constants k_{on} and k_{off} were determined by SPR (see table S1 and S2). For the modelling, the actual **P** feed concentration $[\mathbf{P}]_0 = 6.24\ \mu\text{M}$ was used. The average injected maximum concentration is $[\text{L}]_{max} = 15\ \mu\text{M}$, thus $[\text{L}]_{tot} = 15\ \mu\text{M}$ was chosen. The apparent $K_D(t)$ does not represent the equilibrium but instead the ratio of the species on their way towards equilibrium. Thus, it represents the misinterpretation of the dissociation constant K_D by reading out the species ratio before they reached equilibrium. In the shown experiment, the residence time was 12 s (grey rectangle). Most of the ligands reached a situation insignificantly different from equilibrium. The exceptions are **A23**, with an overestimated K_D of +28%, and **B3**, with an overestimated K_D of +41%. **B16** is not shown because it does not appear to be binding in SPR and consequently k_{on} and k_{off} values are not available.
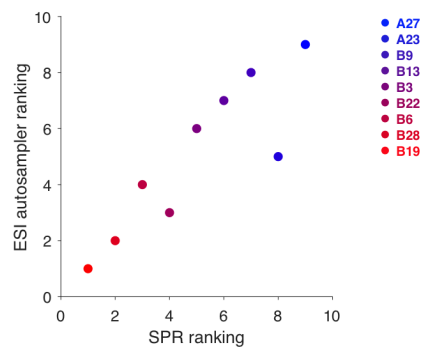
Figure S15. Ligand ranking in the semi-quantitative experiment. The ligands are ranked according to the determined K_D value, i.e., the lowest K_D at rank 1 and the highest K_D at rank 9. This is done for SPR and for the gap sampler. **A23** is out of the trend and **B6** swapped ranking position with **B22**. The other ligands are ranked correctly.
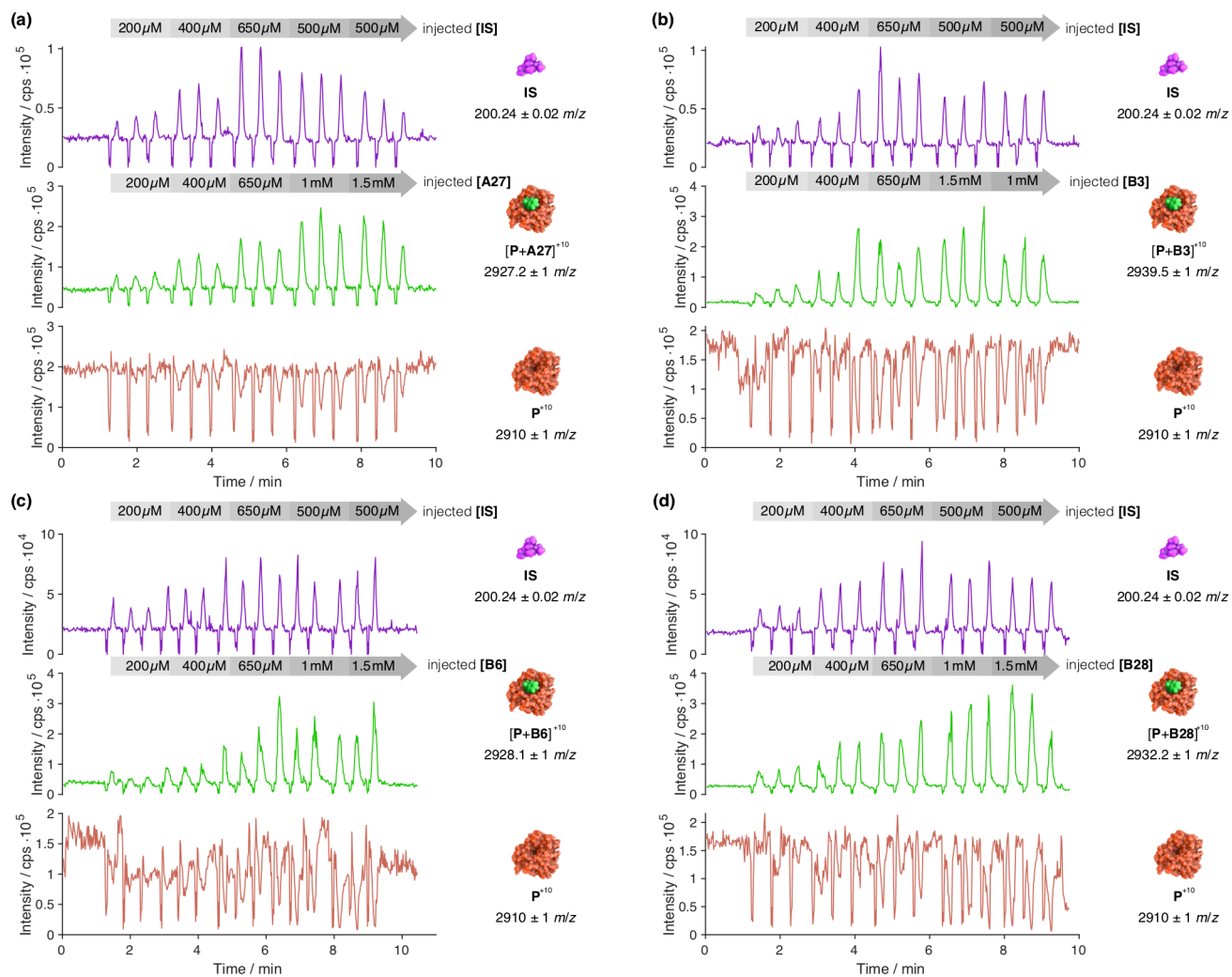
Figure S16. Titration of **A27**, **B3**, **B6** and **B28**. (a) shows the XIC of the **IS** on top. The **IS** concentration on the well plate is listed on the top. The second plot shows the XIC of the complex $[\mathbf{P}+\mathbf{A27}]^{+10}$. The **L** concentration on the well plate is listed on the top. The third plot shows the XIC of the unbound protein $\mathbf{P}^{+10}$. (b) shows the same for **B3**. (c) shows the same for **B6**. (d) shows the same for **B28**.
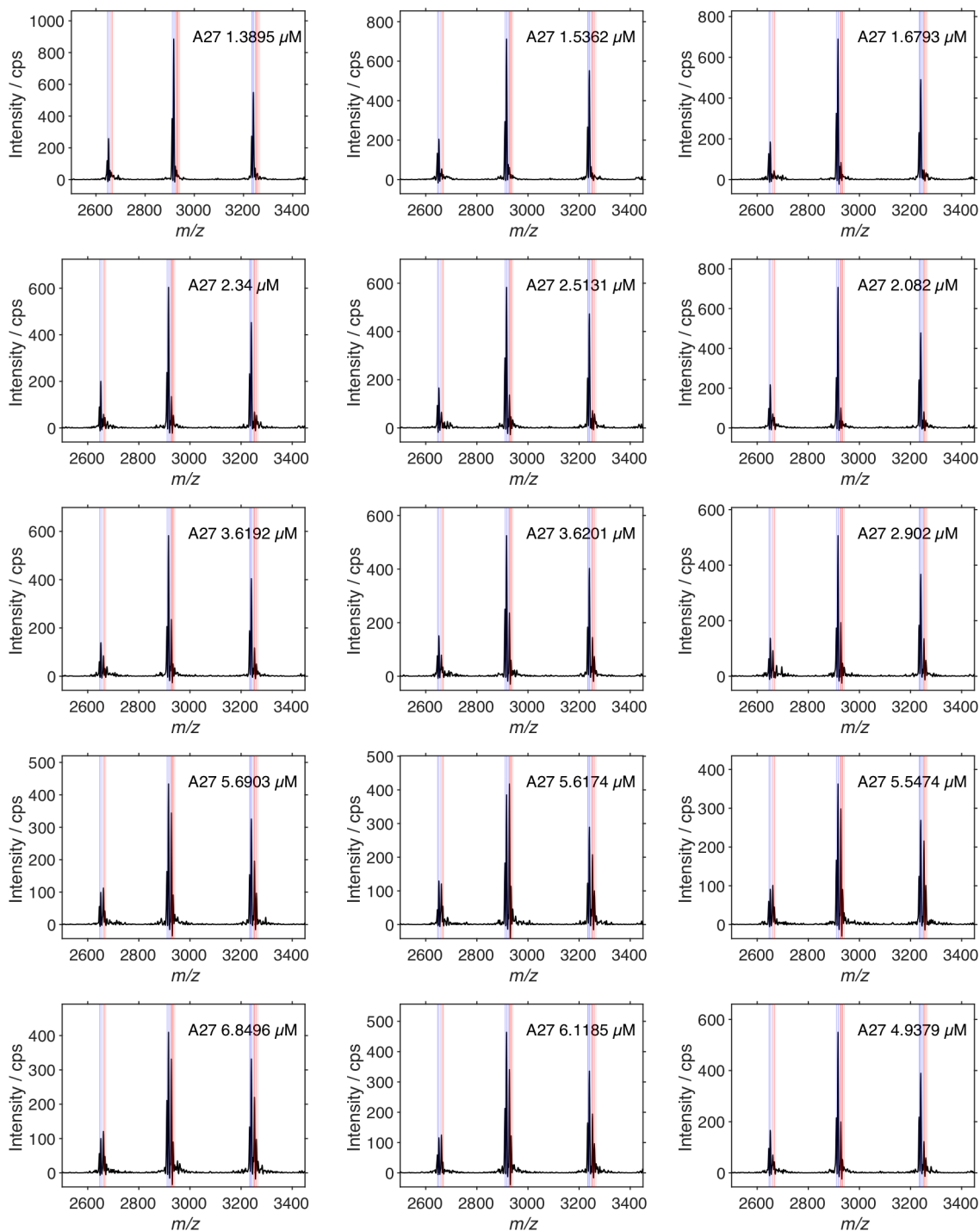
Figure S17. Mass spectra acquired for the titration of the binding ligands **A27**, **B3**, **B6**, **B13** and **B28**. The shown spectra have the highest ratio $\overline{R} = I([\mathbf{P} + \mathbf{Ac}_q + \mathbf{L}]^{n+})/I([\mathbf{P} + \mathbf{Ac}_q]^{n+})$ during one injection cycle (see figure S4), where $q=0,1,2$ are acetate adducts. Thus, the shown spectra are acquired only for 1 s. They were smoothed and baseline subtracted. The red (bound) and the blue (unbound) rectangles mark the integration limits for 11+, 10+ and 9+ charge states of $\mathbf{P}^{n+}$, $[\mathbf{P}+\mathbf{Ac}]^{n+}$, $[\mathbf{P}+\mathbf{Ac}_2]^{n+}$, $[\mathbf{P}+\mathbf{L}]^{n+}$, $[\mathbf{P}+\mathbf{Ac}+\mathbf{L}]^{n+}$ and $[\mathbf{P}+\mathbf{Ac}_2+\mathbf{L}]^{n+}$, which are used to determine the K_D value. On the top right corner, the ligand's label and the determined concentration for the titration point is listed. *Continues on the next page.*
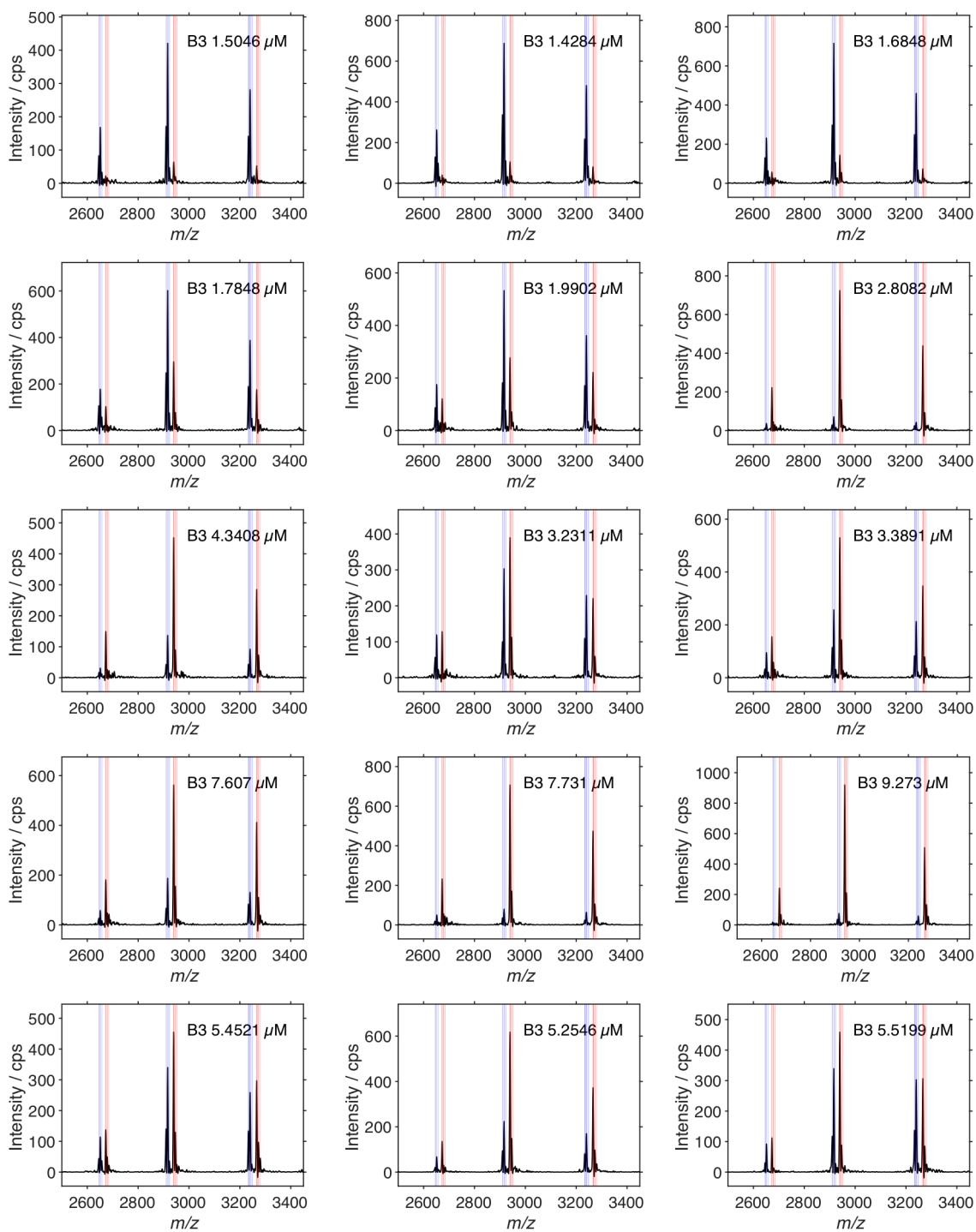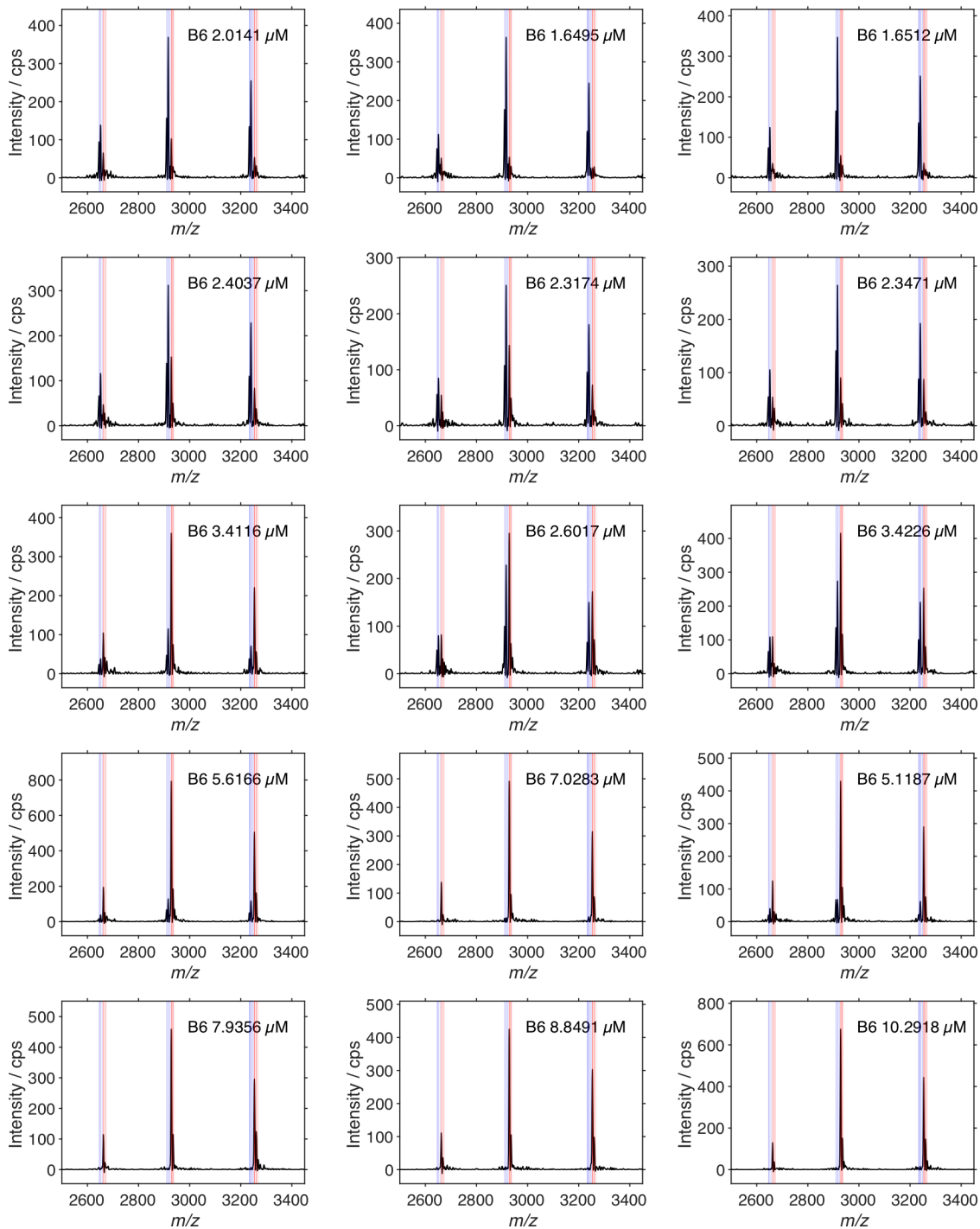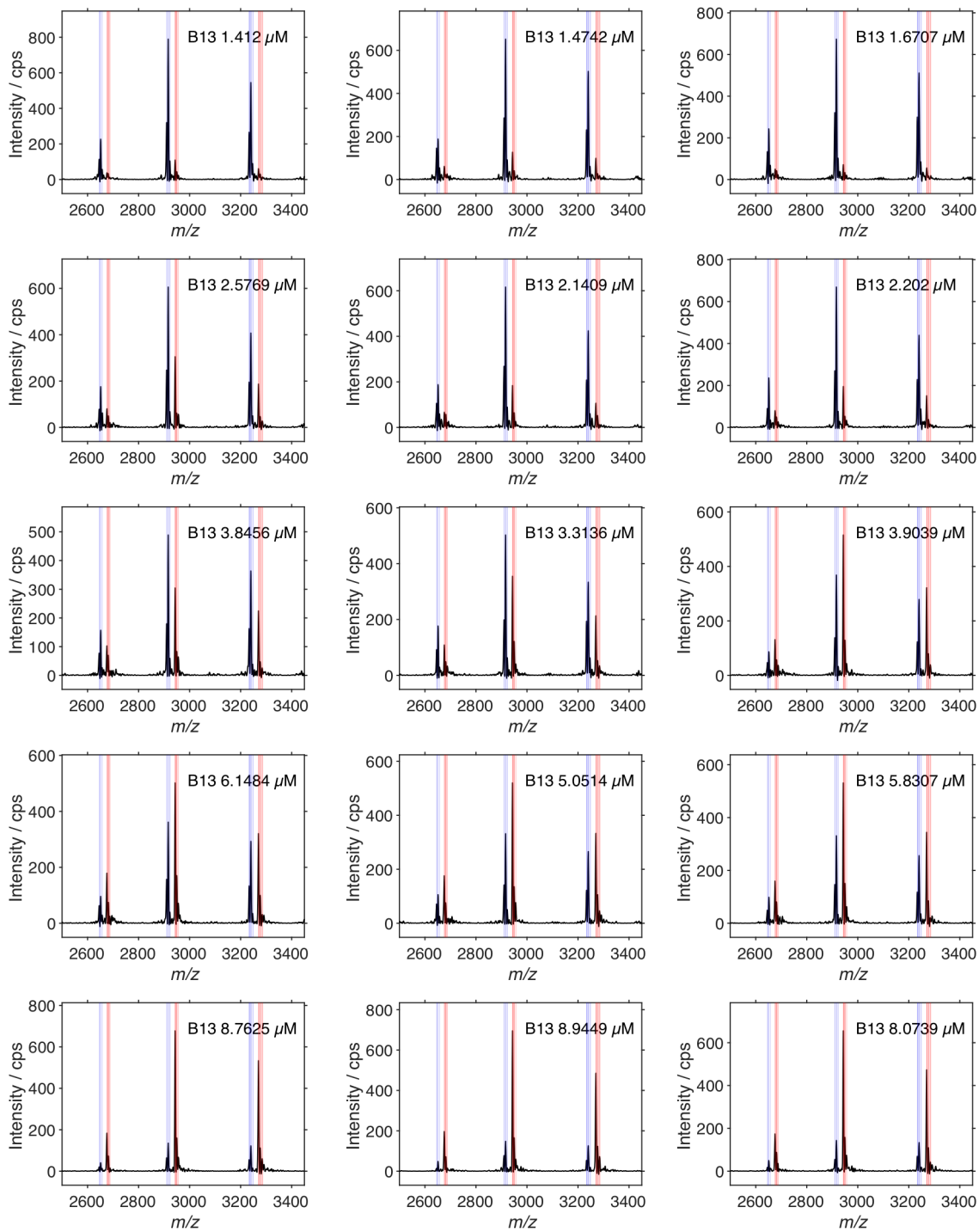
Figure S17. *Continued.*

Figure S17. *Continued.*
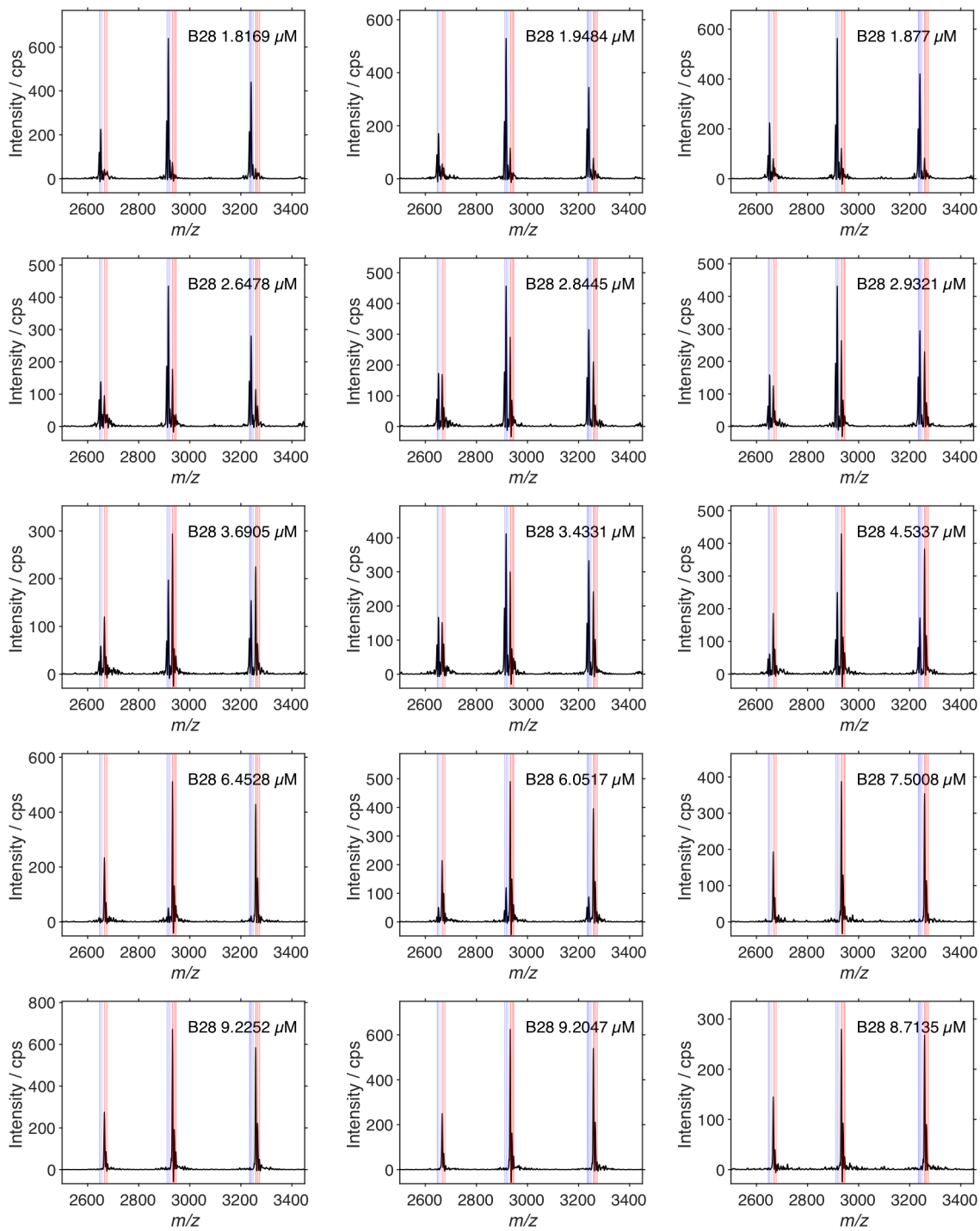
Figure S17. *Continued.*

Figure S17. *Continued.*

References

(1) Neu, V.; Steiner, R.; Muller, S.; Fattinger, C.; Zenobi, R. Development and characterization of a capillary gap sampler as new microfluidic device for fast and direct analysis of low sample amounts by ESI-MS, *Anal. Chem.* **2013**, *85*, 4628-4635.

(2) Zhang, J.-H.; Chung, T. D. Y.; Oldenburg, K. R. A Simple Statistical Parameter for Use in Evaluation and Validation of High Throughput Screening Assays, *J. Biomol. Screen.* **1999**, *4*, 67-73